Cerebral Cortex Advance Access published August 4, 2004

Use of a Recombinant Pseudorabies Virus to Analyze Motor Cortical Reorganization after Unilateral Facial Denervation

Szatmár Horváth[1,2], Emese Prandovszky[1], Eszter Pankotai[1], Zsolt Kis[1], Tamás Farkas[1], Zsolt Boldogköi[3,4], Krisztina Boda[5], Zoltán Janka[2] and József Toldi[1]

[1]Department of Comparative Physiology, Faculty of Science, University of Szeged, H-6726 Szeged, Hungary, [2]Department of Psychiatry, Faculty of Medicine, University of Szeged, Szeged, Hungary, [3]Laboratory of Neuromorphology, Department of Anatomy, Faculty of Medicine, University of Budapest, Budapest, Hungary, [5]Department of Medical Informatics, Faculty of Medicine, University of Szeged, Szeged, Hungary
[4]Present address: Department of Medical Biology, Faculty of Medicine, University of Szeged, Szeged, Hungary

A unilateral facial nerve injury (n7x) was found to influence the transcallosal spread of the attenuated strain of pseudorabies virus (PRV Bartha) from the affected (left) primary motor cortex (MI) to the contralateral MI of rats. We used Ba-DupLac, a recombinant PRV strain, for the tracing experiments since this virus was demonstrated to exhibit much more restricted transportation kinetics than that of PRV Bartha, and is therefore more suitable for studies of neuronal plasticity. Ba-Duplac injection primarily infected several neurons around the penetration channel, but hardly any transcallosally infected neurons were observed in the contraleral MI. In contrast, after right facial nerve injury, Ba-DupLac was transported from the primarily infected neurons in the left MI to the contralateral side, and resulted in the labeling of several neurons due to a transneuronal infection. These results reveal that a peripheral nerve injury induces changes in the Ba-DupLac infection pattern in the related cortical areas. These findings and the literature data suggest that this phenomenon may be related to the changes in the expression or to the redistribution of cell-adhesion molecules, which are known to facilitate the entrance and/or transmission of PRV into neurons.

Keywords: herpes, neuronal plasticity, peripheral nerve injury, primary motor cortex, pseudorabies virus

Introduction

Since the early 1990s, studies demonstrating plasticity in the cortical somatotopic representation maps of the primary motor cortex (MI) of adult animals have brought about a dramatic change in the concept of the function and role of motor cortical areas as information-processing structures (Sanes and Donoghue, 2000). In a series of electrical stimulation mapping experiments, Sanes and Donoghue demonstrated that transection of the facial motor nerve (n7x), which supplies the rat facial whisker musculature, led to a functional loss of the MI whisker area. Consequently, this area was occupied by representations of the adjacent forelimb or eye/eyelid regions (Donoghue *et al.*, 1990; Sanes *et al.*, 1992). This reorganization emerged within hours of the nerve lesion, and persisted for a period of months (Sanes *et al.*, 1990). The earliest sign of motor cortical plasticity induced by n7x can be observed within minutes after the intervention (Toldi *et al.*, 1996, 1999). An important insight into the possible mechanism was revealed by the observation that the blockade of cortical GABAergic inhibition unmasked existing horizontal connections that are probably normally blocked by feed-forward inhibition (Jacobs and Donoghue, 1991). This kind of local GABAergic release yielded map changes parallel to those following nerve lesions, demonstrating that the MI has the intrinsic circuitry necessary to support reorganization, in which the intracortical horizontal connections play a decisive role (Sanes and Donoghue, 2000). Our earlier studies revealed that the motor cortices of both hemispheres, interconnected commissurally, are involved in n7x-induced cortical plasticity (Toldi *et al.*, 1999; Farkas *et al.*, 2000). Most of the studies cited above were based on experiments in which electrophysiological methods were used.

However, it is more than likely that the changes in the cortical representational maps are consequences of molecular biological and biochemical changes in the neurons and the glial cells and in their connections. It has been found, for instance, that n7x leads not only to the activation of astrocytes in the corresponding facial nerve nucleus (Rohlmann *et al.*, 1993, 1994), but also, a few minutes after a peripheral nerve injury, to histochemical and immunohistochemical changes throughout the cortical areas (Negyessy *et al.*, 2000; Hoyk *et al.*, 2002).

Here we demonstrate that the changes induced by n7x in the motor cortical neuronal connections can be studied by neuronal tracing with the pseudorabies virus (PRV).

PRV-Bartha is an attenuated strain of PRV developed as a vaccine (Bartha, 1961). It has been used widely for transneuronal tracing (Enquist *et al.*, 1998; Card, 1999). We used Ba-DupLac, a recombinant PRV strain, for the present tracing experiments, since this virus has been demonstrated to exhibit much more restricted transportation kinetics than that of PRV-Ba (Boldogkoi *et al.*, 2002), and is therefore more suitable for studies of neuronal plasticity. Indeed, we found that the method based on the use of this virus is sensitive enough to detect fine plastic changes induced in the central nervous system by estrogen application (Horvath *et al.*, 2002). In fact, utilization of Ba-DupLac allowed us to reduce the problem to an all-or-none labeling paradigm.

The literature cited above leads us to suppose that n7x induces complex changes, e.g. surface molecule [heparan sulfate-proteoglycan (HSPG) and nectins] redistribution or the gene activation of cortical neurons, which lead to alterations in the functions of their connections. The HSPGs are a group of glycoproteins that carry covalently bound large, unbranched polymers composed of ~20–200 repeating heparin/heparan sulfate disaccharide units, which are usually attached to the core proteins through a serine residue and characteristic carbohydrate linkage regions. It appears that the HSPGs can regulate long-term potentiation (LTP) and may be involved in the morphological maturation of dendritic spines through

multiple ligand interactions; this may be critically dependent on the balance between the different heparin-binding molecules available (Bandtlow and Zimmermann, 2000). Heparan sulfate chains on cell surface proteoglycans also provide initial docking sites for the binding of PRV to eukaryotic cells (Campadelli-Fiume *et al.*, 2000). Nectin-1, a member of the immunoglobulin superfamily, is a component of a novel cell-to-cell adhesion system, localized within the cadherin-catenin system at cell-to-cell adherens junctions (Ajs). It has been shown to play an important role in synapse formation (Mandai *et al.*, 1997; Takahashi *et al.*, 1999; Miyahara *et al.*, 2000; Tachibana *et al.*, 2000; Mizoguchi *et al.*, 2002). Nectin-1 serves as an entry and cell-cell spread mediator of PRV (Geraghty *et al.*, 1998; Campadelli-Fiume *et al.*, 2000).

As concerns our model, the crucial question is whether cell surface molecules exist which can change their expression or distribution following n7x, and which therefore influence the entry of virions into the neurons and/or their cell-to-cell spread.

As the first step, in this study we tested the hypothesis that n7x induces changes in the neuronal connections of the MIs in both hemispheres, which influence the transcallosal PRV labeling pattern.

Materials and Methods

Cells and Virus

A porcine kidney cell line, PK-15, was used for the propagation and titration of PRV. Cells were grown in Dulbecco's modified minimum essential medium (DMEM) supplemented with 5% fetal calf serum at 37°C in a CO_2 incubator. Aliquots of PRV (1000 µl/vial) were stored at -80°C, and single vials were thawed immediately prior to injection. Ba-DupLac was constructed by the insertion of a pair of lacZ expression cassettes to a putative latency promoter (antisense promoter) of PRV-Ba, located in the inverted repeat of the virus (Boldogkoi *et al.*, 2000, 2002).

Animals and Surgical Procedures

The experimental procedures used in this study followed the protocol for animal care approved by the Hungarian Health Committee (1998) and the European Communities Council Directives (86/609/EEC). A total of 28 adult Sprague-Dawley rats were raised with access to water and food pellets (Altromin) *ad libitum*. Sixteen animals were used to study the postinjury/preadministration time (see later and Fig. 2). In 7 of the remaining 12 animals, the right facial nerve trunk was transected 1 h before PRV injection; 5 sham-operated animals served as controls. The nerve cut was made near the stylomastoid foramen. All the surgical procedures were carried out under deep ketamine/xylazine anesthesia (ketamine 10.0 mg/100 g and xylazine 0.8 mg/100 g body wt, i.*P.*).

Injection of the Virus

The head of each rat was fixed in a stereotactic headholder. PRV was injected with special care; the inoculations were made by the same person at the following coordinates: frontal: +2.0 mm to the bregma, lateral 2.0 mm, vertical 800 µm from the cortical surface (Paxinos, 1998). PRV (0.1 µl) was injected over 5 min by pressure (PRV concentration: 10^9 *P.*f.u./ml, vehicle: DMEM + 5% fetal calf serum). The coordinates of the injection site (and of its homotopic point) were determined by prior physiological mapping; we have been carrying out the mapping of MIs since 1996. It is known from the literature (Sanes and Donoghue, 2000) and from our own studies that the injection site (with the coordinates given above) at which intracortical microstimulation induces contralateral whisker movements is in the MI center of the contralateral whiskers (Toldi *et al.*, 1996). The homotopic point in the contralateral hemisphere was determined by intracortical stimulation at the injection site, which transcallosally evoked responses in the homotopic point (Farkas *et al.*, 2000). After determination of the location, and following the completion of the injection, the pipet was left in the tissue for an additional 5 min in order to prevent any backflow of the PRV and/or its spread into the surrounding areas. After the PRV injection, the incision on the head was closed and each animal was housed individually in a plastic isolation cage. The presence and location of PRV-immunoreactive (IR) neurons were checked in all animals. The positions of the tip of the Hamilton syringe and the lesion induced by the PRV injection were verified histologically in cresyl violet-stained sections.

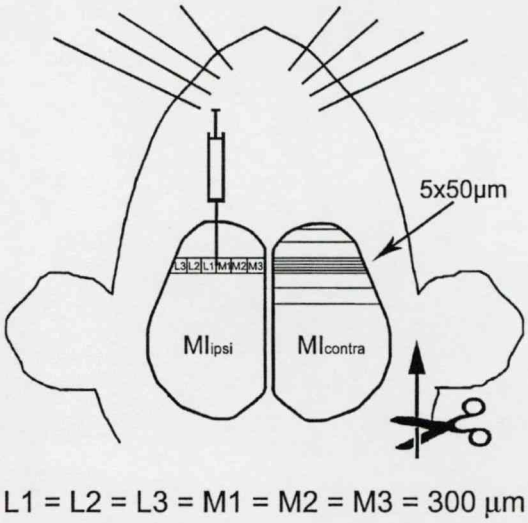

Figure 1. A schematic drawing to explain the experimental paradigm. PRV was injected into the whisker representation area in the left motor cortex (MIipsi). PRV-immunoreactive (PRV-IR) neurons were counted in five consecutive 50 µm wide coronal sections of both hemispheres (as shown in the right hemisphere: MIcontra). To facilitate the analysis, the photomicrographs of the five coronal sections (forming the 250 µm wide bands of the cortices) were divided in the mediolateral direction into six 300 µm wide areas (on the coronal surface): L1 = L2 = L3 = M1 = M2 = M3 = 300 µm. The numbers of PRV-IR cells obtained in five sham-operated and five n7x animals were quantified according to this cortical division. In one animal each in both the sham-operated and the n7X group, serial sections (50 µm wide) of the rostral part of both hemispheres were made (also as shown in the right hemisphere: MIcontra). The PRV-IR neurons were counted in every sixth section in these two animals. The three-dimensional distributions of the PRV-IR neurons in Figure 5 were constructed on the basis of these studies. Scissors plus arrow denotes the right side facial nerve cut. The divisions (L3–M3 in the left hemisphere, the labeling of the 50 µm wide cortical slides and the mark of every sixth section in the rostral half of the right hemisphere) serve only for demonstration and, of course, are not proportionate in this schematic drawing.

Perfusion and Immunocytochemistry

After survival for 72 h, the animals were deeply anesthetized as described above and perfused transcardially with ~200 ml of phosphate-buffered saline (PBS, 0.1 mol/l, pH 7.3), followed by ~200 ml of Zamboni's fixative (2.0% aqueous paraformaldehyde solution — from a 16% stock solution containing 15% picric acid — in 0.1 M sodium phosphate buffer stock, pH 7.3) (Stefanini *et al.*, 1967). Brains were postfixed in fresh Zamboni's solution overnight. Coronal sections (50 µm thick) of the brain were cut using a Vibratome (Campden Instruments) and were processed for PRV immunocytochemistry. Only those animals were evaluated ($n = 10$) in which the infection was successful, i.e. infected neurons (PRV-IR) were seen in the left motor cortex and the whole length of the penetration channel was situated within the cortex. The sections were blocked in 5% normal goat serum (diluted in PBS) for 1 h, and incubated with a rabbit polyclonal antibody (Rb133; 1:10 000, courtesy of Professor L.W. Enquist, Department of Molecular Biology, Princeton University, Princeton, NJ, USA) overnight at 4°C. The sections were then treated with biotinylated anti-rabbit IgG (1:200, Vector Laboratories) for 2 h at room temperature. The immunohistochemical reaction was visualized with the ABC-DAB technique

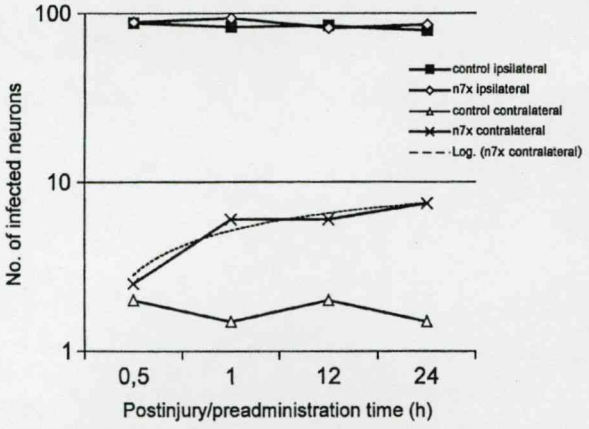

Figure 2. The number of infected neurons increased logarithmically with the postinjury/preadministration time only in the right hemisphere of the n7x animals (n7x contralateral; its log fit is depicted by a broken line). The other three curves are linear and parallel to the *x*-axis. The postinjury/preadministration time on the abscissa means that PRV was injected into the animals 0.5 h ($n = 2$), 1 h ($n = 2$), 12 h ($n = 2$) or 24 h ($n = 2$) after n7x. The study was also made on eight sham-operated animals. The PRV infection was followed in each case by a 72 h survival time.

(ABC-Elite Kit, Vector Laboratories); sections were mounted on gelatinized slides, dehydrated and coverslipped with Entellan® (Merck).

Statistical Analysis

To prevent experimental bias, the facial nerve status was decoded for statistical analysis after cell counts had been collected. In our experiments, five consecutive (50 μm thick) coronal sections from both hemispheres of the animals were processed for PRV immunocytochemistry. Accordingly, in both hemispheres, all of the PRV-IR neurons within these 250 μm wide bands of the MIs were encountered. In the left hemisphere, this 250 μm wide cortical band contained the penetration channel too (Fig. 1). To check whether the infection pattern exceeded the 250 μm wide band, one animal randomly selected from the n7x group and one from the sham-operated group were treated and processed as described previously, but serial sections of the rostral part of the hemispheres were made. In these cases, we selected every sixth section for data sampling (Figs 1 and 5). We used the nonparametric Mann-Whitney *U*-test to analyze the difference between the total number of infected cells on each cortical side in the control and n7x groups. Repeated-measures ANOVA was applied to test the mean effects on the number of infected cells and the interactions between the facial nerve status (between-subject), the cortical side (within-subject) and the cortical area (within-subject). The slides were processed digitally (Olympus BX51, DP11, Camedia Master 2.0). The coronal sections of the motor cortices were then divided into six 300 μm wide areas on the cortical surface (Figs 1 and 4), making the infection pattern easier to analyze. Statistical analysis was performed with the aid of the SPSS 11.0 for Windows program. The results are expressed as means ± SD; $P < 0.05$ was regarded as significant.

Data Presentation in Figures

The PRV-IR neurons in Figrue 3 are shown in microphotographs. In Figure 4, diagrams of coronal sections were constructed to demonstrate in two dimensions the distribution and localization pattern of PRV-IR cells observed within 250 μm wide bands of both cortices of five controls and five n7x animals. Since the differences in the numbers of labeled neurons within the detailed studied 250 μμm wide bands in the five slides were very small, the average number of labeled neurons in a slide could be calculated and given (see the small SDs in Fig. 4). In these drawings, the motor cortical slices were divided into 300 μm wide areas. The black areas denote the medial and lateral areas closely adjacent to the injection channel. The gray areas are homotopic to them. In Figure 5, the schematic surface diagrams depict in three dimensions the distribution of PRV-IR neurons in the frontal part of both hemi-

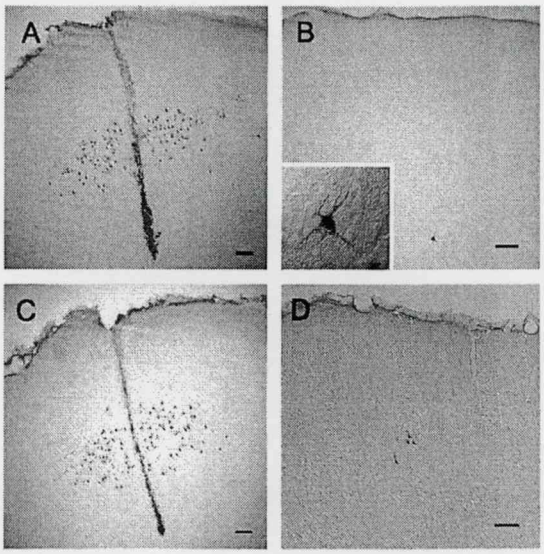

Figure 3. Labeled neurons in the left (*A*) and right (*B*) primary motor cortices (MIs) of a control animal, and in the left (*C*) and right (*D*) primary motor cortices of a rat in which the right facial nerve was transected 1 h before the PRV infection. Several PRV-infected neurons are localized around the injection channels (*A*, *C*). We could not usually observe labeling in the contralateral MI of the controls (*B*), with some exceptions, where a few labeled cells were detected. Inset in *B*: higher magnification of the one labeled pyramidal neuron found in this control animal. (*A* and *B* are corresponding slides.) (*D*) PRV-IR neurons in the homotopic area of the right hemisphere of an n7x animal, after facial denervation. Calibration: 100 μm in *A–D*. In the inset in *B*, the bar is 10 μm.

spheres of a sham-operated and of an n7x animal. L1, L2 and L3 denote the three 300 μm wide bands on the cortical surface lateral to the injection site. M1, M2 and M3 denote the three 300 μm wide bands on the cortical surface medial to the injection site. O1, O2 and O3 denote the three 300 μm wide bands on the cortical surface in the oral direction from the injection site. C1, C2 and C3 denote the three 300 μm wide bands on the cortical surface caudal to the injection site (see also Fig. 1).

Results

n7x Influences the Transcallosal Spread of PRV in a Time-dependent Manner

To determine whether the peripheral injury of the nervous system has a virus immunohistochemically detectable effect on the synaptic connections, the right facial nerve of the animals was cut or the animals were sham-operated before administration of the PRV suspension. Synaptic reorganization can reveal viral glycoprotein receptors or can induce other protein–protein interactions, which can modulate the entry or transmission of viral particles. We were interested in determining the time course of the possible reorganization, and we therefore applied different postinjury/preadministration times. The results obtained with PRV are shown in Figure 2. The postinjury/preadministration duration did not have a significant effect on the inoculation side in either group. On the contralateral side of the injured animals (n7x contralateral in Fig 2), the number of infected neurons increased in a time-dependent manner. The number reached a plateau at ~1 h postinjury/preadministration. In the sham-operated animals, there was no significant effect of the resting time (control contralateral and control ipsilateral in Fig 2). It is likely that the changes in the motor cortex affect the neuronal transmission of PRV in a short period, i.e. within 1 h.

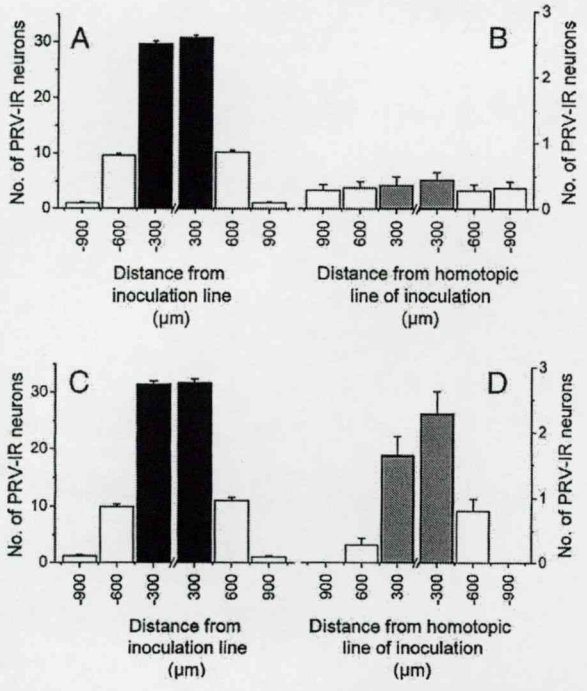

Figure 4. Schematic diagrams of the distribution of labeled cells in two slides of controls (*A, B*) and in two slides of n7x animals (*C, D*). The average number of labeled cells per slide is given in these diagrams. The averages of the cell numbers were calculated from the corresponding data on five controls and five n7x animals, i.e. from 5 × 5 slides. The motor cortices are divided into 300 μm wide areas (see also Fig. 1). The black areas denote the 300 μm wide cortical areas in the close medial and lateral environment of the injection channel in the left hemispheres (*A, C*). The gray areas are homotopic to them in the right hemispheres (*B, D*). Values are means and SDs for PRV-IR neurons ($n = 25$) (see also Fig. 1).

PRV Immunoreactivity Was not Different on the Inoculation Side in the Controls and the n7x Animals

To examine the effects of n7x on the entry and/or cell-to-cell spread of PRV, we compared the numbers and distributions of infected cells on the inoculation side of the cerebral cortex. The primarily infected neurons were found around the penetration channel in both the controls and the n7x animals (Fig. 3*A,C*). In all cases, the primarily infected neurons were located discretely in the third lamina of the motor cortex. This is consistent with the selective uptake of the virus by the middle-layer cells. The highest number of labeled neurons was found close to the injection channel, and the number decreased with increasing distance from this. These results seem to be consistent with the diffusion of PRV-containing solution around the cannula.

There was no significant difference between the control and n7x groups in the number of labeled neurons (82.3 ± 3.36 versus 86.2 ± 3.82; $P = 0.119$), or in the infection patterns on the injected side (Figs 3*A,C* and 4*A,C*). These results indicate that the entry of PRV into the motor cortical neurons is not dependent on facial denervation.

PRV Immunoreactivity Differs in the Contralateral MI in the Controls and the n7x Animals

To test whether n7x affects the cell-to-cell spread of PRV, we compared the numbers and distributions of infected cells in the cortex contralateral to the inoculation. The transcallosally infected cells displayed cytoplasmic staining (as shown in Fig 3*B*, inset), and by 72 h following inoculation strong PRV immunoreactivity could be seen in these neurons. In the control animals, there were significantly fewer labeled neurons in the contralateral (right side) cerebral cortex than in the n7x animals (2.0 ± 1.86 versus 5.0 ± 1.83; $P < 0.001$ (see Figs 3*B–D* and 4*B,D*). In the n7x animals, these neurons were located close to the homotopic line of the injection channel (Fig. 4*D*). n7x not only increased the number of transcallosally labeled neurons, but also affected their distribution. ANOVA indicated a significant three-way interaction between the facial nerve status, the cortical side and the cortical area [$F(5,40) = 15.64$, $P < 0.0001$], i.e. the mean of the PRV-IR cell number is dependent on the cortical side, the cortical area and the unilateral n7x.

In the control animals, the distributions of the transcallosally infected neurons were identical in the divided cortical areas (Fig. 4*B*). There was no significant difference between the divided areas in the number of labeled neurons.

Although we did not perform a detailed study, in the course of a rough survey, PRV-IR neurons were not found in any other cortical area (e.g. in the somatosensory cortex) apart from the motor cortices on both sides.

The Motor Cortex Is Homogenous for Viral Spread in Both Mediolateral and Orocaudal Directions

To confirm that this infection pattern does not exist in only two dimensions, one animal randomly selected from each group was treated and processed as described previously, and serial sections of the brains were made. The surface diagrams of the distribution of the PRV-IR neurons revealed a cone-like shape on the ipsilateral side in both groups (Fig. 5*A,C*) and also on the contralateral side in the n7x animals (Fig. 5*D*). On the contralateral side of the sham-operated animal, the diagram was nearly planar (Fig. 5*B*). A possible explanation is the diffusion of the viral suspension on the inoculation side — the farther from the injection channel, the lower the probability of infected neurons. Envelope proteins of PRV and other herpes viruses play an essential role in target cell recognition, attachment and receptor-mediated fusion of virions to permissive profiles. Additionally, some envelope proteins exhibit an affinity for extracellular matrix molecules such as HSPG that are present in the extracellular milieu of the nervous system. These affinities act to limit the diffusion of virions from the injection site and thereby contribute to the ability to carry out localized injections of PRV. Finally, the large size of the PRV particle may further aid in limiting the diffusion of injected tracer (Enquist *et al.*, 1998; Aston-Jones and Card, 2000). In this case, it means that at least this part of the cerebral cortex is homogenous concerning viral infection.

On the contralateral side of the control animal, the distribution of infected neurons was uniform (Fig. 5*B*), which means that the neurons around the infection channel received afferents from all parts of the contralateral side. After n7x, this afferentation was more focused; the surface diagram exhibited a distribution of PRV-IR neurons similar to that observed on the inoculation side (Fig. 5*D*).

These results indicate that the transcallosal cell-to-cell spread of PRV within the MIs of both hemispheres is influenced by n7x.

Discussion

The present study has demonstrated that n7x influences the transcallosal spread of PRV from the MI on the affected side to

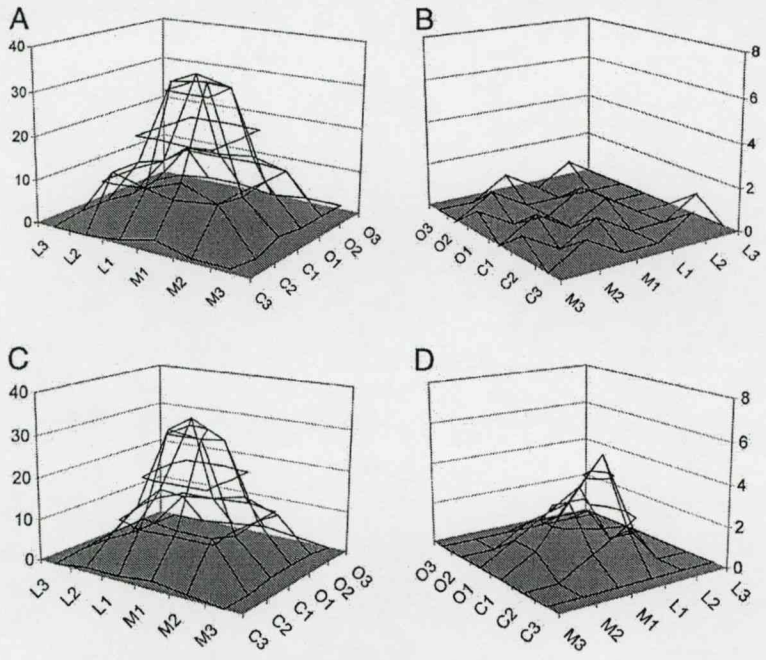

Figure 5. Surface diagrams for a sham-operated (*A*, *B*) and n7x animal (*C*, *D*). The diagrams exhibit a cone-like shape, which demonstrates the distribution of PRV-IR neurons on the inoculation side (*A*, *C*). In contrast, the diagram of the contralateral cortex is virtually planar (*B*), while in the right hemisphere of the n7x animal there is an impressive peak in the surface diagram at the homotopic point of the injection channel (*D*). It should be mentioned that the distance of sampling was in 300 μm in the mediolateral direction, but 50 μm in the rostrocaudal direction in these animals.

the contralateral MI in rats. The main observations were as follows: in the controls, PRV injection primarily infected several neurons around the penetration channel, but hardly any transcallosally infected neurons were found in the contralateral MI. In coronal sections, these neurons exhibited an almost constant distribution from medial to lateral in the cerebral cortex. In contrast, after right n7x, PRV was transported from the primarily infected neurons in the left MI to the contralateral side, and resulted in the labeling of several neurons via transneuronal infection. These transcallosally labeled neurons were concentrated near the homotopic line of the injection channel. The number of infected neurons reached a plateau 1 h postinjury/preadministration.

In our tracing study, we did not find any other infected brain areas associated with a motor function apart from the MIs. In the MIs, the interhemispheric connections between the homotopic representation fields of the vibrissal muscles undergo rapid disinhibition (minutes after denervation) (Toldi *et al.*, 1999; Farkas *et al.*, 2000). The question arises of whether this disinhibition of interhemispheric connections might play a role in the observed enhanced transcallosal labeling. Our results suggest that a new transcallosal path is unmasked quickly after the peripheral n7x. In adult rats, the MI exhibits a noteworthy capacity to react to peripheral nerve lesions, with changes in the perisynaptic glia and synaptic reorganization, with latencies of from 1 h up to 1 day. The results we have presented here also show that the changes in the motor cortex affect the neuronal transmission of PRV within 1 h. Our results, supported by statistical analysis, suggest that n7x not only facilitates, but also augments the transcallosal spread of PRV from the left MI to the contralateral side. Unilateral n7x did not affect the entry of PRV into the neurons (infected primarily).

To explain this result, it should be taken into account that the entry of alpha herpes viruses into the cells usually requires multiple interactions between the viral envelope and the cell surface proteins. At least two groups (HSPGs and nectins) of these cell surface (glyco)proteins are known to play roles in these processes (Mettenleiter, 2000; Spear *et al.*, 2000). It should also be considered that HSPGs and nectins participate in the development and plasticity in adulthood of tissues of neuroepithelial origin (Carey, 1997; Rauvala and Peng, 1997; Suzuki *et al.*, 2000; Mizoguchi *et al.*, 2002).

Our present results suggest that n7x does not affect the entry of PRV, but increases the efficiency of its cell-to-cell spread. Thus, we may speculate that the n7x-dependent infection pattern appears to be related not to cellular components (HSPGs) involved in the attachment of the virus, but rather to cellular components located in the synaptic region of the membrane of presynaptic neurons.

Many articles (see the review by Sanes and Donoghue, 2000) or our own results (Toldi *et al.*, 1999; Farkas *et al.*, 2000) demonstrate that n7x induces changes in cortical activity in extended areas. On the basis of these results, we suggest that, as a consequence of these changes in cortical activity (or in parallel with them), changes also take place in the expression of the cell surface molecules in the presynaptic terminals of transcallosal axons of motor cortical origin on the right side. Accordingly, we consider that the virus transport in our experiments was mainly transynaptic and retrograde. There are additional indications in support of retrograde transport. (i) In the course of our experiments, we never observed labeled axon terminals in the right hemisphere. This also holds for the retrograde transport. (ii) The firmest evidence is the recent observation by Enquist and co-workers (Enquist *et al.*, 2002;

Pickard *et al.*, 2002) that PRV-Bartha was transported transynaptically only in the retrograde direction (i.e. from postsynaptic to presynaptic neuron).

The suggested relationship between the n7x-induced changes in cortical activity and the changes in the neuronal surface molecules is further supported, and partially explained, by recent results indicating that the expression of the cell surface molecules which we suggest might play roles in the retrograde, trans-synaptic cell-to-cell spread of PRV is controlled dynamically and locally, and modulated by synaptic activity (Tanaka *et al.*, 2000) or via activity-dependent regulatory pathways (Pierre *et al.*, 2001; Murase *et al.*, 2002).

However, in addition to the adhesion molecule (nectin-1α)-aided cell-to-cell spread of the virus (Sakisaka *et al.*, 2001), its enhanced direct uptake and retrograde axonal transport into the contralateral hemisphere after n7x cannot be completely excluded either. With regard to the enhanced number of PRV-IR neurons in the contralateral primary motor cortex after n7x, due either to trans-synaptic retrograde cell-to-cell spread or to direct uptake and retrograde transport of the virus, the role of the cell adhesion molecules in these processes is hardly disputable.

Nectin-1 and nectin-2, components of a novel cell-to-cell adhesion system, and localized within the cadherin–catenin system at cell-to-cell Ajs, have been shown to play an important role in synapse formation (Mandai *et al.*, 1997; Takahashi *et al.*, 1999; Miyahara *et al.*, 2000; Tachibana *et al.*, 2000; Mizoguchi *et al.*, 2002). The synaptic scaffolding molecule (S-SCAM) is localized at the Ajs in the CA3 area of the hippocampus in a nectin-dependent manner. This finding indicates that S-SCAM serves as a scaffolding molecule at the Ajs after maturation of the synapses and at the synaptic junctions during the maturation. S-SCAM is a neural scaffolding protein which interacts with many proteins, including *N*-methyl-D-aspartic acid (NMDA) receptors (Yamada *et al.*, 2003). The nectin–afadin system may be involved in the structural changes that occur at synapses during the maintenance phase of LTP by modulating the redistribution of synaptic components.

The remodeling of cortical circuits (including new synapse formation) might also play a part in the plasticity of the motor cortex, which contains both the substrate (the horizontal connection system) and the mechanisms (LTP and long-term depression) for reorganization after peripheral nerve injury (Sanes and Donoghue, 2000). The mechanism by which n7x increases the efficiency of cell-to-cell spread or the direct uptake of PRV in the cortical network *in vivo* remains to be elucidated, but the dense and focused PRV-IR suggests changes in the background (in cell surface molecules), which should be of significance in the cortical reorganization after a peripheral nerve injury. We have recently started to study this aspect of cortical plasticity.

Whatever the underlying mechanism is, the peripheral nerve injury-induced changes in the Ba-DupLac infection pattern seem to be a suitable model for the study of injury-induced neuronal plasticity. Such studies reveal another aspect of peripheral nerve injury-induced cortical reorganization.

Notes

The authors thank Professor L.W. Enquist (Department of Molecular Biology, Princeton University, Princeton, NJ, USA) for the gift of the primary antiserum. The research was supported by grants from the National Research Foundation (OTKA T031893, T046687 and M36213). T.F. and Z.K. are Békésy György Postdoctoral fellows (BÖ 211/2001 and BÖ 163/2002).

Address correspondence to J. Toldi, Department of Comparative Physiology, University of Szeged, POB 533, H-6726 Szeged, Hungary. Email: toldi@bio.u-szeged.hu.

References

Aston-Jones G, Card JP (2000) Use of pseudorabies virus to delineate multisynaptic circuits in brain: opportunities and limitations. J Neurosci Methods 103:51–61.

Bandtlow CE, Zimmermann DR (2000) Proteoglycans in the developing brain: new conceptual insights for old proteins. Physiol Rev 80: 1267–1290.

Bartha A (1961) Experimental reduction of virulence of Aujeszky's disease virus. Magy Allatorv Lapja 16:42–45.

Boldogkoi Z, Erdelyi F, Fodor I (2000) A putative latency promoter/enhancer (P(LAT2)) region of pseudorabies virus contains a virulence determinant. J Gen Virol 81:415–420.

Boldogkoi Z, Reichart A, Toth IE, Sik A, Erdelyi F, Medveczky I, Llorens-Cortes C, Palkovits M, Lenkei Z (2002) Construction of recombinant pseudorabies viruses optimized for labeling and neurochemical characterization of neural circuitry. Brain Res Mol Brain Res 109:105–118.

Campadelli-Fiume G, Cocchi F, Menotti L, Lopez M (2000) The novel receptors that mediate the entry of herpes simplex viruses and animal alphaherpesviruses into cells. Rev Med Virol 10:305–319.

Card JP EL (1999) Transneuronal circuit analysis with pseudorabies virus. In: Current protocols in neuroscience (Crawley JN GC, McKay R, Rogawski MA, Sibley DR, Skolnick P, eds). New York: Wiley.

Carey DJ (1997) Syndecans: multifunctional cell-surface co-receptors. Biochem J 327(pt 1):1–16.

Donoghue JP, Suner S, Sanes JN (1990) Dynamic organization of primary motor cortex output to target muscles in adult rats. II. Rapid reorganization following motor nerve lesions. Exp Brain Res 79:492–503.

Enquist LW, Husak PJ, Banfield BW, Smith GA (1998) Infection and spread of alphaherpesviruses in the nervous system. Adv Virus Res 51:237–347.

Enquist LW, Tomishima MJ, Gross S, Smith GA (2002) Directional spread of an alpha-herpesvirus in the nervous system. Vet Microbiol 86: 5–16.

Farkas T, Perge J, Kis Z, Wolff JR, Toldi J (2000) Facial nerve injury-induced disinhibition in the primary motor cortices of both hemispheres. Eur J Neurosci 12:2190–2194.

Geraghty RJ, Krummenacher C, Cohen GH, Eisenberg RJ, Spear PG (1998) Entry of alphaherpesviruses mediated by poliovirus receptor-related protein 1 and poliovirus receptor. Science 280: 1618–1620.

Horvath S, Kis Z, Boldogkoi Z, Nogradi A, Toldi J (2002) Oestrogen-dependent tracing in the rat CNS after pseudorabies virus infection. Eur J Neurosci 15:937–943.

Hoyk Z, Varga C, Parducz A (2002) Transneuronal induction of the highly sialylated isoform of the neural cell adhesion molecule following nerve injury. Acta Biol Hung 53:67–75.

Jacobs KM, Donoghue JP (1991) Reshaping the cortical motor map by unmasking latent intracortical connections. Science 251:944–947.

Mandai K, Nakanishi H, Satoh A, Obaishi H, Wada M, Nishioka H, Itoh M, Mizoguchi A, Aoki T, Fujimoto T, Matsuda Y, Tsukita S, Takai Y (1997) Afadin: a novel actin filament-binding protein with one PDZ domain localized at cadherin-based cell-to-cell adherens junction. J Cell Biol 139:517–528.

Mettenleiter TC (2000) Aujeszky's disease (pseudorabies) virus: the virus and molecular pathogenesis — state of the art, June 1999. Vet Res 31:99–115.

Miyahara M, Nakanishi H, Takahashi K, Satoh-Horikawa K, Tachibana K, Takai Y (2000) Interaction of nectin with afadin is necessary for its clustering at cell-cell contact sites but not for its cis dimerization or trans interaction. J Biol Chem 275:613–618.

Mizoguchi A, Nakanishi H, Kimura K, Matsubara K, Ozaki-Kuroda K, Katata T, Honda T, Kiyohara Y, Heo K, Higashi M, Tsutsumi T, Sonoda S, Ide C, Takai Y (2002) Nectin: an adhesion molecule involved in formation of synapses. J Cell Biol 156:555–565.

Murase S, Mosser E, Schuman EM (2002) Depolarization drives beta-catenin into neuronal spines promoting changes in synaptic structure and function. Neuron 35:91-105.

Negyessy L, Gal V, Farkas T, Toldi J (2000) Cross-modal plasticity of the corticothalamic circuits in rats enucleated on the first postnatal day. Eur J Neurosci 12:1654-1668.

Paxinos GW (1998) The rat brain in stereotaxic coordinates, 4th edn. San Diego, CA: Academic Press.

Pickard GE, Smeraski CA, Tomlinson CC, Banfield BW, Kaufman J, Wilcox CL, Enquist LW, Sollars PJ (2002) Intravitreal injection of the attenuated pseudorabies virus PRV Bartha results in infection of the hamster suprachiasmatic nucleus only by retrograde transsynaptic transport via autonomic circuits. J Neurosci 22:2701-2710.

Pierre K, Dupouy B, Allard M, Poulain DA, Theodosis DT (2001) Mobilization of the cell adhesion glycoprotein F3/contactin to axonal surfaces is activity dependent. Eur J Neurosci 14:645-656.

Rauvala H, Peng HB (1997) HB-GAM (heparin-binding growth-associated molecule) and heparin-type glycans in the development and plasticity of neuron-target contacts. Prog Neurobiol 52:127-144.

Rohlmann A, Laskawi R, Hofer A, Dobo E, Dermietzel R, Wolff JR (1993) Facial nerve lesions lead to increased immunostaining of the astrocytic gap junction protein (connexin 43) in the corresponding facial nucleus of rats. Neurosci Lett 154:206-208.

Rohlmann A, Laskawi R, Hofer A, Dermietzel R, Wolff JR (1994) Astrocytes as rapid sensors of peripheral axotomy in the facial nucleus of rats. Neuroreport 5:409-412.

Sakisaka T, Taniguchi T, Nakanishi H, Takahashi K, Miyahara M, Ikeda W, Yokoyama S, Peng YF, Yamanishi K, Takai Y (2001) Requirement of interaction of nectin-1alpha/HveC with afadin for efficient cell-cell spread of herpes simplex virus type 1. J Virol 75:4734-4743.

Sanes JN, Donoghue JP (2000) Plasticity and primary motor cortex. Annu Rev Neurosci 23:393-415.

Sanes JN, Suner S, Donoghue JP (1990) Dynamic organization of primary motor cortex output to target muscles in adult rats. I. Long-term patterns of reorganization following motor or mixed peripheral nerve lesions. Exp Brain Res 79:479-491.

Sanes JN, Wang J, Donoghue JP (1992) Immediate and delayed changes of rat motor cortical output representation with new forelimb configurations. Cereb Cortex 2:141-152.

Spear PG, Eisenberg RJ, Cohen GH (2000) Three classes of cell surface receptors for alphaherpesvirus entry. Virology 275:1-8.

Stefanini M, De Martino C, Zamboni L (1967) Fixation of ejaculated spermatozoa for electron microscopy. Nature 216:173-174.

Suzuki K, Hu D, Bustos T, Zlotogora J, Richieri-Costa A, Helms JA, Spritz RA (2000) Mutations of PVRL1, encoding a cell-cell adhesion molecule/herpesvirus receptor, in cleft lip/palate-ectodermal dysplasia. Nat Genet 25:427-430.

Tachibana K, Nakanishi H, Mandai K, Ozaki K, Ikeda W, Yamamoto Y, Nagafuchi A, Tsukita S, Takai Y (2000) Two cell adhesion molecules, nectin and cadherin, interact through their cytoplasmic domain-associated proteins. J Cell Biol 150:1161-1176.

Takahashi K, Nakanishi H, Miyahara M, Mandai K, Satoh K, Satoh A, Nishioka H, Aoki J, Nomoto A, Mizoguchi A, Takai Y (1999) Nectin/PRR: an immunoglobulin-like cell adhesion molecule recruited to cadherin-based adherens junctions through interaction with afadin, a PDZ domain-containing protein. J Cell Biol 145:539-549.

Tanaka H, Shan W, Phillips GR, Arndt K, Bozdagi O, Shapiro L, Huntley GW, Benson DL, Colman DR (2000) Molecular modification of N-cadherin in response to synaptic activity. Neuron 25:93-107.

Toldi J, Laskawi R, Landgrebe M, Wolff JR (1996) Biphasic reorganization of somatotopy in the primary motor cortex follows facial nerve lesions in adult rats. Neurosci Lett 203:179-182.

Toldi J, Farkas T, Perge J, Wolff JR (1999) Facial nerve injury produces a latent somatosensory input through recruitment of the motor cortex in the rat. Neuroreport 10:2143-2147.

Yamada A, Irie K, Deguchi-Tawarada M, Ohtsuka T, Takai Y (2003) Nectin-dependent localization of synaptic scaffolding molecule (S-SCAM) at the puncta adherentia junctions formed between the mossy fibre terminals and the dendrites of pyramidal cells in the CA3 area of the mouse hippocampus. Genes Cells 8:985-994.

ELSEVIER

Neuroscience Letters 358 (2004) 223–225

Neuroscience Letters

www.elsevier.com/locate/neulet

Facial nerve injury induces facilitation of responses in both trigeminal and facial nuclei of rat

Zsolt Kis, Gabriella Rákos, Tamás Farkas, Szatmár Horváth, József Toldi*

Department of Comparative Physiology, University of Szeged, Közép fasor 52, H-6726 Szeged, Hungary

Received 10 September 2003; received in revised form 16 January 2004; accepted 19 January 2004

Abstract

A study was made of the effects of facial nerve transection on trigeminal stimulation- evoked field potentials in the principal trigeminal (Pr5) and facial nuclei (7) in rats. Although the transected branch of the facial nerve contains pure motoric efferents, it resulted in enhanced responses in both Pr5 and 7. These electrophysiological results suggest a functional circuitry involving the whiskers, trigeminal nerve, Pr5 and 7 and the facial nerve as efferent. The disconnection (opening) of this loop results in enhanced responsiveness of the neurons in both Pr5 and 7.

Keywords: Vibrissa sensorimotor system; Functional loop; Trigeminal nerve; Facial nerve; Principal trigeminal nucleus; Facial nucleus; Plasticity

Neurophysiological studies have revealed that peripheral nerve manipulation alters the topography of somatotopic representation maps in both the somatosensory [1] and the motor cortices [13]. Following transection of the facial nerve trunk or the branches innervating the vibrissal muscles, for example, the cortical representations of the forelimb and eye/eyelid muscles become enlarged and expand into the interposed facial nerve field. These plastic changes have been observed to develop during some days after a nerve injury [3,13].

We have reported transient but rapid changes (developing during a few minutes) in the primary motor cortex of the rat after facial nerve lesions [16]. Analysis revealed that these cortical plastic changes were based on injury-induced disinhibition [5], which uncovered latent inputs in the motor cortex, resulting in cortical representational plasticity [15].

These results lead to the question of how the motor cortex is so rapidly 'informed' of the injury to the facial nerve. As an explanation, a loop functioning between the whiskers and the central nervous system is presumed, in which the afferent is the infraorbital branch of the trigeminal nerve, while the efferent is the pure motoric postauricular branch of the facial nerve. The loop is probably closed on more than one level. At a cortical level, the importance of the associative connections between the primary somatosensory and motor cortices in these plastic changes has already been studied [4].

In the present experiments, we studied a presumed loop closing at a hindbrain level in order to learn (i) whether whisker stimulation evokes responses in the facial nucleus, (ii) whether axotomy influences these responses, and (iii) whether facial nerve injury influences the whisker stimulation-evoked responses in the trigeminal nucleus.

The experimental procedures used in this study followed the protocol for animal care approved by the European Communities Council Directives (86/609/EEC). In addition to nine sham-operated rats (the right facial nerve was exposed, but not cut), 12 littermates were studied at the age of 60–80 days. They were anesthetized with a mixture of Ketavet (10.0 mg/100 g) and Rompun (xylasine, 0.8 mg/100 g). The right facial nerve, including its postauricular branch, was exposed, and during the experiments (recordings) was transected (N7X) near the stylomastoid foramen. The anesthetized animals were secured in a stereotaxic head holder (David Kopf) that provided access to the facial nucleus (7) or brainstem trigeminal principal nucleus (Pr5). After surgery, the animals were allowed to rest for 1 h. The core temperature was maintained at 37 ± 0.3 °C. The whisker pad was stimulated with bipolar needle electrodes (0.5 Hz, 0.3 ms, 100–150 μA). Under stereotaxic guidance, evoked responses were recorded with a glass micropipette filled with 2.5 M NaCl (impedance 2–7 MΩ). The electrodes were advanced in 3–5-μm steps by means of a Narishige hydraulic micromanipulator. The signals were fed into a differential amplifier with 1 Hz lower and 5 kHz upper frequency limits, and visualized on a Tektronix storage oscilloscope. Amplified responses were fed into a computer

* Corresponding author. Tel.: +36-62-544153; fax: +36-62-544291.
E-mail address: toldi@bio.u-szeged.hu (J. Toldi).

0304-3940/03/$ - see front matter © 2004 Elsevier Ireland Ltd. All rights reserved.
doi:10.1016/j.neulet.2004.01.037

via an interface (Digidata 1200, pClamp 6.0.4. software, Axon Instruments) and stored for further processing. In statistical analysis (unpaired two-tailed *t*-test), averages of 3×20 evoked potentials were used. For details of the stimulation, recording, data processing and response properties evoked by vibrissa pad stimulation, see [7,15].

After the experiments, the animals were fixed by transcardial perfusion with 4% paraformaldehyde in 0.1 M phosphate buffer. The brains were removed and the site of the recording electrode was verified in cresyl violet-stained coronal sections made with a Vibratome.

The experimental paradigm is shown in Fig. 1. Right-side whisker pad stimulation (STIM) evoked responses ipsilaterally in both Pr5 and 7. In Pr5, the complex response has components ***a***, ***b***, ***c*** and ***d*** (Fig. 2A1). The response properties observed in Pr5 were discussed in detail earlier [7]. However, this is the first study of the effects of N7X on the responses evoked in Pr5 by trigeminal activation. Although the injured branch of the facial nerve contains pure motoric fibers [14], its injury resulted in increasing amplitudes of component ***b*** of the response in Pr5 (Fig. 2A2,B). Facilitation of component ***b*** was observed in five of six animals.

The whisker pad stimulation also evoked complex responses (field potentials) in the facial nucleus (7) with a ***b***-peak latency of 3.2 ± 1.5 ms (Fig. 3A1). Component ***a*** of the response (probably the antidromic component) was stable in amplitude and latency, but components ***b***, ***c*** and ***d*** in most cases, and especially in the lateral part of the facial nucleus, proved sensitive to the facial nerve cut. The most

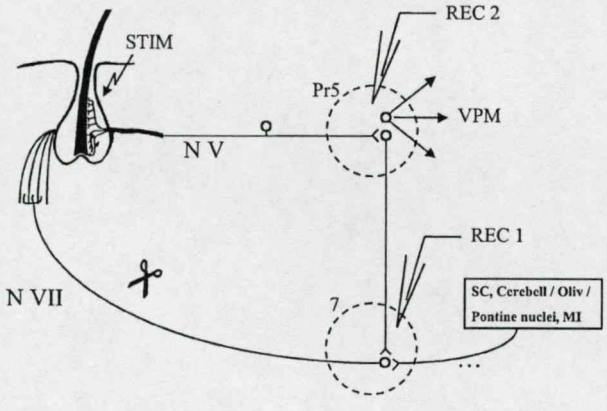

Fig. 1. The whisker pad, the infraorbital nerve, the principal nucleus (Pr5), the facial nucleus (7) and the facial nerve form a functional circuitry (a functional loop; see [6]). By cutting the facial nerve (N7X), we opened this functional loop. The experimental paradigm: a part of the trigeminal system (N V) (infraorbital nerve) was activated by stimulation of the right-side whisker pad (STIM). The evoked field potentials were recorded ipsilaterally, either in the facial nucleus (7, REC 1) or in the trigeminal principal nucleus (Pr5, REC 2). The effects of a facial nerve cut were studied on the whisker pad stimulation-evoked responses in 7 or Pr5. SC, superior colliculus. Cerebell (cerebellar), Oliv (olivary), Pontine nuclei and the MI (primary motor cortex) are the main midbrain, cerebellar and cortical inputs of 7. Arrows at Pr5: symbolic outputs of Pr5, including VPM (ventral posteromedial nucleus of the thalamus).

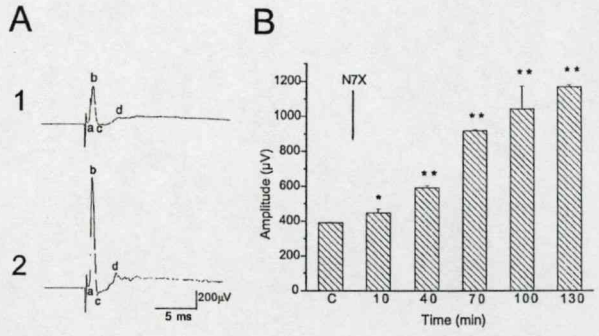

Fig. 2. An example of the whisker pad stimulation-evoked averaged response (20 responses were averaged) and its changes in Pr5. (A1) Electrical stimulation of the whisker pad evoked complex field potentials in Pr5, of which component ***b*** was sensitive to the facial nerve cut (N7X). (A2) Averaged response with facilitated component ***b*** observed 100 min after N7X. (B) The amplitude of component ***b*** (measured from peak ***a*** to peak ***b***) was greatly facilitated after N7X. Ordinate: amplitude of component ***b*** before (C) and 10, 40, 70, 100 or 130 min after N7X. $*P < 0.05$; $**P < 0.01$ (unpaired two-tailed *t*-test; $n = 3$, i.e. 3×20 potentials, amplitudes are mean ± S.D.).

sensitive component of the response was ***b*** (Fig. 3A2). After N7X, component ***b*** of the infraorbital nerve stimulation-evoked responses in 7 increased (in some cases enormously) in amplitude. These plastic changes took 30–50 min to develop (Fig. 3B). In two of six animals, N7X did not influence the whisker pad stimulation-evoked responses in 7. The N7X-induced facilitation of component ***b*** of the responses was recorded mainly in the lateral subdivision of 7, but we were unable to establish a clear and firm relationship between the recording site and the facilitation.

Earlier studies have demonstrated that N7X rapidly induces transient changes in large parts of both hemispheres. Electrophysiologically, the most marked change is the facilitation of the motor cortex responses to stimulation of the unilateral infraorbital nerve [15]. It has emerged that these changes are based on cortical disinhibition [5]. The question

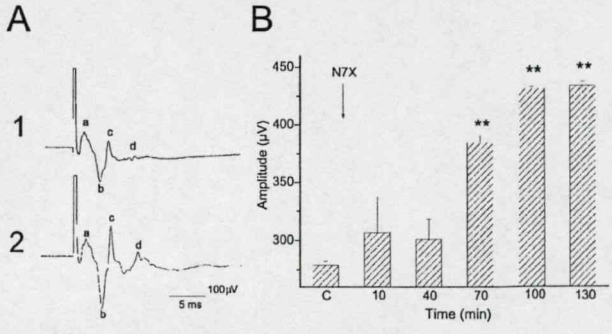

Fig. 3. An example of the whisker pad stimulation-evoked response (20 responses were averaged) and its changes in 7. (A1) Electrical stimulation of the whisker pad evoked complex field potentials in the facial nucleus with several components, of which component ***b*** was extremely sensitive to the facial nerve cut (A2). (B) The amplitude of component ***b*** (measured from peak ***a*** to peak ***b***) was greatly facilitated after N7X. Ordinate: amplitude of component ***b*** before (C) and 10, 40, 70, 100 or 130 min after N7X. $**P < 0.01$ (unpaired two-tailed *t*-test; $n = 3$, i.e. 3×20 potentials, amplitudes are mean ± S.D.).

arose as to whether these plastic changes are specific to the cortex or are also detectable in subcortical structures. A decade ago, morphological evidence was presented suggesting that synaptic reorganization in 7 begins within less than 1 h after N7X [11,12]. However, N7X induced motor cortical electrophysiological changes within 4 min [16]. Because of the short latency, it was suggested that the facial nerve injury probably induces a process mediated by the somatosensory system, leading to disinhibition in the motor cortices of both hemispheres [15]. These data suggested a closed loop(s?) functioning between the whiskers and the central nervous system. We earlier analyzed the afferent (trigeminal) elements [7], and the closing of this loop at a cortical level [4,5,15]. We have now studied the question of whether a closed loop functions at a hindbrain level.

A positive answer can be given to all the questions put forward in the introduction. Whisker pad stimulation evoked responses not only in Pr5, but also in 7. N7X influenced the evoked field potential activity not only in 7, but in Pr5 too. Anatomical studies [17] lead us to speculate that N7X near the stylomastoid foramen results in axotomy of the neurons mainly in the lateral subdivision of 7. It has been shown that retrograde injury factors resulting from axotomy are able to alter the membrane properties and thus the excitability of facial motoneurons [10]. It is also possible that some part of the facial nucleus is activated antidromically by vibrissal pad stimulation. Such activation could leave some facial neurons refractory before their activation through the trigeminal loop. After N7X, such antidromic inactivation would not be possible and this could also account for the facilitation in 7. The N7X-induced changes in the evoked field potentials in 7 might be explained in these ways, but not the facilitation observed in Pr5. The only explanation is the loop presumed to be functioning in the hindbrain (see Fig. 1). We suggest that disconnection (opening) of the loop would result in enhanced excitability not only in 7 but also in other elements of the loop, e.g. Pr5.

The anatomical, behavioral and electrophysiological evidence that has accumulated allows us to identify neuronal circuitries involved in vibrissa-mediated sensation and the control of rhythmic vibrissa movement [2,6,8,9]. Here we present electrophysiological evidence for a loop closing at a hindbrain level.

The role of these loops in the control of whisking has been well studied [8,9], but further experiments are needed to provide an understanding of these processes, and especially the mechanism and the importance of these plastic changes in the reorganization following the injury (opening) of these closed loops.

Acknowledgements

This work was supported by OTKA grant T031893. T.F. and Z.K. were recipients of Békésy György postdoctoral fellowships (BÖ 211/2001 and BÖ 163/2002).

References

[1] M.B. Calford, Dynamic representational plasticity in sensory cortex, Neuroscience 111 (2002) 709–738.
[2] M. Deschenes, E. Timofeeva, P. Lavallee, The relay of high-frequency sensory signals in the Whisker-to-barreloid pathway, J. Neurosci. 23 (2003) 6778–6787.
[3] J.P. Donoghue, S. Suner, J.N. Sanes, Dynamic organization of primary motor cortex output to target muscles in adult rats. II. Rapid reorganization following motor nerve lesions, Exp. Brain Res. 79 (1990) 492–503.
[4] T. Farkas, Z. Kis, J. Toldi, J.R. Wolff, Activation of the primary motor cortex by somatosensory stimulation in adult rats is mediated mainly by associational connections from the somatosensory cortex, Neuroscience 90 (1999) 353–361.
[5] T. Farkas, J. Perge, Z. Kis, J.R. Wolff, J. Toldi, Facial nerve injury-induced disinhibition in the primary motor cortices of both hemispheres, Eur. J. Neurosci. 12 (2000) 2190–2194.
[6] A.M. Hattox, C.A. Priest, A. Keller, Functional circuitry involved in the regulation of whisker movements, J. Comp. Neurol. 442 (2002) 266–276.
[7] Z. Kis, T. Farkas, K. Rabl, E. Kis, K. Kóródi, L. Simon, I. Marusin, J. Toldi, Comparative study of the neuronal plasticity along the neuraxis of the vibrissal sensory system of adult rat following unilateral infraorbital nerve damage and subsequent regeneration, Exp. Brain Res. 126 (1999) 259–269.
[8] D. Kleinfeld, R.W. Berg, S.M. O'Connor, Anatomical loops and their electrical dynamics in relation to whisking by rat, Somatosens. Mot. Res. 16 (1999) 69–88.
[9] S.M. O'Connor, R.W. Berg, D. Kleinfeld, Coherent electrical activity between vibrissa sensory areas of cerebellum and neocortex is enhanced during free whisking, J. Neurophysiol. 87 (2002) 2137–2148.
[10] T. Patko, I. Vassias, P.P. Vidal, C. De Waele, Modulation of the voltage-gated sodium- and calcium-dependent potassium channels in rat vestibular and facial nuclei after unilateral labyrinthectomy and facial nerve transection: an in situ hybridization study, Neuroscience 117 (2003) 265–280.
[11] A. Rohlmann, R. Laskawi, A. Hofer, R. Dermietzel, J.R. Wolff, Astrocytes as rapid sensors of peripheral axotomy in the facial nucleus of rats, NeuroReport 12 (1994) 409–412.
[12] A. Rohlmann, R. Laskawi, A. Hofer, E. Dobo, R. Dermitzel, J.R. Wolff, Facial nerve lesions lead to increased immunostaining of the astrocytic gap junction protein (connexin 43) in the corresponding facial nucleus of rats, Neurosci. Lett. 154 (1993) 206–208.
[13] J.N. Sanes, J.P. Donoghue, Plasticity and primary motor cortex, Annu. Rev. Neurosci. 23 (2000) 393–415.
[14] K. Semba, M.D. Egger, The facial 'motor' nerve of the rat: control of vibrissal movement and examination of motor and sensory components, J. Comp. Neurol. 247 (1986) 144–158.
[15] J. Toldi, T. Farkas, J. Perge, J.R. Wolff, Facial nerve injury produces a latent somatosensory input through recruitment of the motor cortex in the rat, NeuroReport 10 (1999) 2143–2147.
[16] J. Toldi, R. Laskawi, M. Landgrebe, J.R. Wolff, Biphasic reorganisation of somatotopy in the primary motor cortex follows facial nerve lesions in adult rats, Neurosci. Lett. 203 (1996) 179–182.
[17] J.B. Travers, Oromotoric nuclei, in: G. Paxinos (Ed.), The Rat Nervous System, 2nd Edition., Academic Press, San Diego, CA, 1994, pp. 239–255.

ELSEVIER

Neuroscience Letters 342 (2003) 49–52

Neuroscience Letters

www.elsevier.com/locate/neulet

Peripheral nerve injury influences the disinhibition induced by focal ischaemia in the rat motor cortex

Tamás Farkas[a], Enikő Racekova[b], Zsolt Kis[a], Szatmár Horváth[a], Jozef Burda[b], Jan Galik[b], József Toldi[a,*]

[a]*Department of Comparative Physiology, University of Szeged, Közép fasor 52, H-6726 Szeged, Hungary*
[b]*Institute of Neurobiology, Slovak Academy of Sciences, Kosice, Slovakia*

Received 4 February 2003; accepted 12 February 2003

Abstract

Photothrombotic lesions were produced in the rat primary motor cortex, and the brain excitability was assessed in a paired-pulse stimulation protocol by transcranial recording, in parallel at 16 points of the frontal cortex, including the insulted and the surrounding areas. The cortical lesion reduced the inhibition in the extended frontal cortex, with a delay of a few minutes. Unilateral facial nerve transection, however, accelerated the widespread disinhibition. Although the mechanism is not clear in detail, both peripheral and central injury-induced disinhibition may have a significant impact on the recovery of the function.

Keywords: Nerve injury; Cortical disinhibition; Focal ischaemia; Rose Bengal; Motor cortex; Facial nerve

It is well known that both deafferentation of a sensory cortex [2] and deefferentation of the primary motor cortex (MI) [13] induce a reduction in cortical inhibition, during which different types of cortico-cortical connections are modulated in efficacy. The functional meaning of such a change is still obscure, but its importance is unquestionable from both theoretical and clinical aspects (mention may be made of phantom pain and synkinesia).

No less interesting and important a topic is the ischaemia-induced plastic changes in the cortex (we may consider stroke). Schiene et al. [14] recently described an enlargement of the cortical vibrissa representation in the surroundings of an ischaemic cortical lesion. Extended brain disinhibition has been demonstrated following an ischaemia-induced focal cortical lesion [1].

Both denervation and ischaemia-induced cortical changes indicate that widespread remote decreases in inhibition are a common feature of these peripheral and central injuries.

Among the questions that may arise, the most important one is how these remote effects favour or impair the recovery of function. As the first step in the investigation of this complex problem, in the present work we have examined whether the two manipulations interact or not in causing disinhibition.

The experimental procedures used in this study followed the protocol for animal care approved by the European Communities Council Directives (86/609/EEC). A total of 30 Sprague–Dawley adult rats of either sex were anaesthetized with i.p. injections of a mixture of Ketavet (10.0 mg/100 g) and Rompun (xylasine, 0.8 mg/100 g). The rats were placed into a stereotaxic frame and the skull was exposed. On the left side, above the MI, the skull was thinned with a dental drill from about 2 mm posterior to 5 mm anterior of the bregma, and from 0.5 to 5 mm lateral of the midline. In the course of the operation, we also exposed the right side facial nerve (n7), including its postauricular branch. The cortical photothrombotic (pt) lesion was carried out by i.v. injection of Rose Bengal (1.3 mg/100 g) and cold light exposure, as described by Buchkremer-Ratzmann and Witte [1]. There were two main groups of animals: the controls ($n = 10$) and the lesioned animals ($n = 20$). In the ten controls, either illumination was applied ($n = 4$) or Rose Bengal was given without cold light application ($n = 3$). In three animals, neither Rose Bengal nor light exposure was applied. In three of the 20 lesioned rats, only a pt lesion was

* Corresponding author. Tel.: +36-62-544153; fax: +36-62-544291.
E-mail address: toldi@bio.u-szeged.hu (J. Toldi).

0304-3940/03/$ - see front matter
doi:10.1016/S0304-3940(03)00230-1

carried out, while in 17 rats, the pt lesion was combined with the transection of n7 (n7X). In four of the 17 animals, the pt lesion was followed by n7X immediately, before the electrophysiological recordings. In 13 animals, the n7X was carried out with a 30 min delay, during the electrophysiology. Since GABAergic inhibition is stable at low frequency (<0.1 Hz, see Ref. [4]), in nine animals in this group, the vibrissa pad stimulation was given at 0.05 Hz, while in all other cases 1 Hz stimulation was applied, as tried in our own earlier in vivo studies [5]. In all experiments, transcranial multichannel recordings (without skull opening) were used.

During the electrophysiological study, the right vibrissa pad was stimulated with a bipolar needle electrode (150–250 μA) to induce evoked potentials (EPs) in the MI. Amplified responses were fed into a computer via an interface (Digidata 1200, pClamp 6.0.4. software, Axon Instruments) and stored for further processing. For details of stimulation, recording, data processing and response properties evoked in the MIs by peripheral somatosensory stimulation, see Ref. [15].

A paired-pulse stimulation protocol was applied to investigate paired-pulse inhibition or facilitation effects on the amplitudes of the EPs. Field potentials were recorded transcranially, in parallel in 16 channels, using tungsten electrodes in a matrix of 4 × 4 mm over the left MI (Fig. 1A). Averaged amplitudes of three or 60 EPs during 1 min periods (corresponding to 0.05 and 1 Hz, respectively) were observed before and after the intervention (Fig. 2), and were computed for all 16 channels. In these experiments, the ratio of the EP amplitudes elicited by the second versus the first stimulus was calculated ($Q = EP_2/EP_1$). Values of $Q < 1$ indicate that the second response was inhibited by the first. More details concerning the in vivo paired-pulse stimulation-evoked responses in the MI, and the observations on cortical inhibition and facilitation, are to be found in Ref. [5].

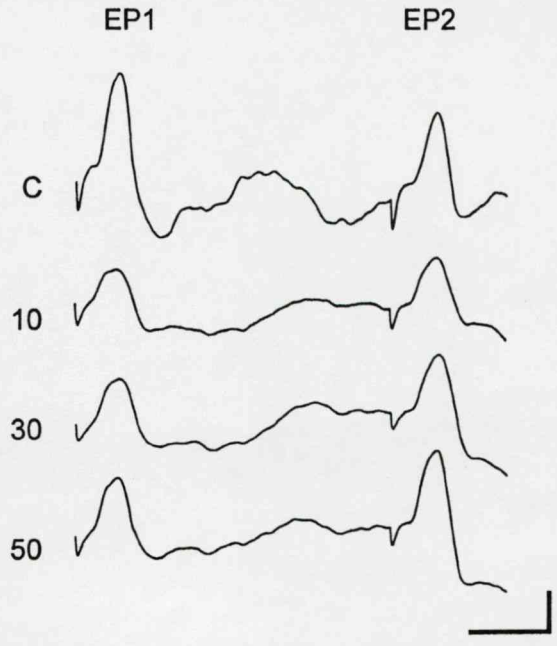

Fig. 2. Averaged amplitudes of field potentials evoked by paired-pulse trigeminal stimulation. Potentials were recorded in the primary motor cortex (see star in Fig. 1A) before (C) and 10, 30 and 50 min after the photothrombotic lesion. Calibration: 50 min, 200 μV.

Routine light microscopic analysis was carried out on animals surviving for 2 h or 2 days following the pt lesion, and also on the control rats. The deeply anaesthetized (sodium pentobarbital 80 mg/kg, i.p.) animals were perfused transcardially with saline, followed by 4% paraformaldehyde in 0.1 M phosphate buffer (pH 7.4). The brains were removed from the skull, postfixed in the same fixative and cryoprotected in 30% sucrose. Frozen 40 μm thick sections were cut serially in the coronal plane and processed according to the Gallyas reduced silver method for degenerating neurones [6].

The control animals showed no evidence of pathological

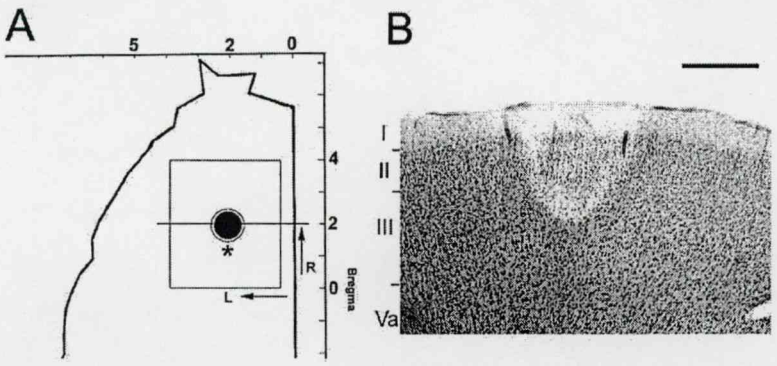

Fig. 1. Exact localization of lesions and the site of electrophysiological recordings in the frontal cortex of the rat. (A) The photothrombotic lesion was produced at the following co-ordinates: frontal, 2–3 mm; lateral, 2 mm. Transcranial electrophysiological recordings were carried out at 16 points within the matrix shown in the figure. The filled circle represents the centre of the core, which was surrounded by the penumbra (open circle). The sizes of both (core and penumbra) changed with time. The histologically detectable penumbra developed with a delay of a few days. (B) Brain coronal section made as indicated with a horizontal line in (A). The photomicrograph shows a damaged cortex region as early as 2 h after the beginning of the photothrombotic lesion. The section was processed according to the Gallyas method. L, lateral; R, rostral. Calibration: 500 μm.

changes in the brain tissue. No one animal from the three different control groups exhibited any histological alteration. In the pt-lesioned animals, after 2 h, the ischaemia had caused well-observable damage 800–1000 μm in diameter in the brain tissue, which was typical after 2 h of survival (Fig. 1B). The tissue of the contralateral hemisphere was never involved; normal-appearing cells and pale neurones were observed.

The present study focused on the early electrophysiological events that took place in the cortex during the first 2 h after illumination. The recorded 4 × 4 mm area in the MI is shown in Fig. 1A. Right-side whisker pad stimulation (at either 0.05 or 1 Hz) evoked responses in the entire left MI, with amplitudes of 200–500 μV. The punctum maximum of the EPs in the MI on contralateral whisker pad stimulation was localized 2–2.5 mm rostral to the bregma and 2.0–2.5 mm lateral to the midline. In the controls, and in all the treated animals before the intervention, a double pulse stimulation study (see details in Ref. [5]) indicated a rather strong paired-pulse inhibition, with Q values of 0.3–0.5 (Fig. 3A and inset in Fig. 4). A few minutes after the pt lesion, the amplitudes of the EPs were dramatically reduced. Although the amplitudes of the EPs in the MI were reduced 5–10 min after the pt lesion, the Q values calculated on the basis of the double pulse stimulation protocol suggested an increased level of disinhibition throughout the entire cortical area. After the pt lesion, the elevated Q values varied in time, but they were always around or above 1 (Fig. 3B and the first 25 min in Fig. 4), and persisted at this high level during the studied period of 2–2.5 h. Similar results were observed in all animals, independently of the stimulation frequency applied.

Interesting results were obtained in previously pt-lesioned animals, in which n7X was carried out with a 30 min delay. In these animals, the Q values were observed before and after n7X, as detailed earlier. However, a 'general' level of inhibition-excitation was expressed by the Q_a value, which represents the actual inhibition-excitation level in the entire 4 × 4 mm cortical area during the respective 5 min period (see details in Fig. 4). In these animals, the Q_a values were around 1 because of the previous pt lesion; these values were further increased by n7X (Fig. 4). The time-dependent pattern of the changes in Q_a is similar to that of the changes induced by pure n7X [5], except for the much higher Q_a values. Similar time-dependent patterns of the changes in Q_a were found in all 13 animals stimulated at either 0.05 or 1 Hz.

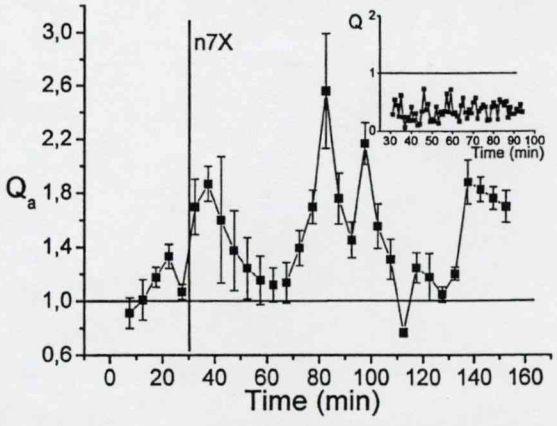

Fig. 4. An example of the change in the 'averaged' Q values (Q_a) in time. These Q_as represent the means of Q values (with SD) calculated from the paired responses observed at 16 points of the recorded area of an animal which underwent the photothrombotic lesion previously, before the electrophysiological recording (see the high level of Q_as (around 1) at the beginning, due to the photothrombotic lesion). After facial nerve transection (vertical line with n7X), the Q_a values further increased. Inset: diagram of the ratio (Q) of the paired response amplitudes evoked by right whisker pad stimulation in a control animal, in relation to time (min). It should be noted that the Q values in the primary motor cortex of a control rat were always below 1 (around 0.3–0.5). See details in Ref. [5].

The present experiments provide further support for the data obtained by means of electrophysiological studies showing that both focal lesions in the motor cortex [1] and n7X [5,15,16] induce transient and widespread disinhibition in both, but especially in the insulted hemisphere. In addition, it is shown that the disinhibition induced by a previous focal lesion can be further enhanced by n7X.

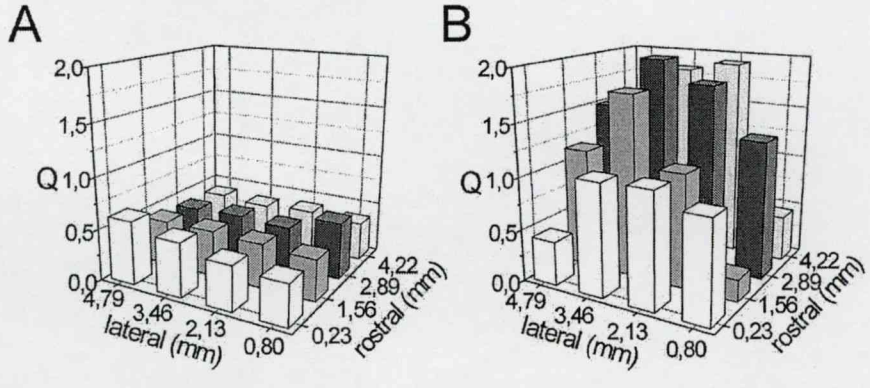

Fig. 3. Q values calculated from paired-pulse stimuli-evoked averaged potentials recorded at 16 points in the frontal cortex of an animal. (A) Q values before pt lesion. (B) Q values calculated from potentials recorded 40 min after the pt lesion.

In the present study, we focused on the early electrophysiological events. However, it should be noted that the cortical lesion elicits post-lesion repetitive episodes of peri-infarct depolarizations during the first 10–30 min [8], which reduce the synaptic excitation and inhibition, and therefore might have disturbed our observations. To avoid these early misleading effects, we followed the electrophysiological recordings for some hours after the intervention. Although the mechanism of injury-induced cortical disinhibition is still obscure, the studies indicate that decreases in GABAergic inhibition are a common feature of focal ischaemic cortical injuries [1,9]. Similarly, peripheral nerve injury also led to decreased GABAergic inhibition [2,13].

The mechanism of decrease in GABAergic inhibition is still not clear in all details, but recently published results of an in vitro study demonstrated that ischaemia caused an adenosine-mediated inhibition of the GABAergic synaptic transmission, which was coupled with an increased paired-pulse facilitation [3]. Other mechanisms may also have roles in this phenomenon, e.g. the dysregulation of the GABA(A) receptor subunit [12] or the reverse GABA effect: excitatory actions of GABA were found after neuronal trauma [17]. Interestingly, Cl^--accumulating cells were observed in axotomized neurones, this finding fitting in well with the findings of a reverse GABA effect [11].

However, besides disinhibition, strong facilitation was occasionally observed in the paired-pulse paradigm, after pt lesion + n7X. In the dentate gyrus, the paired-pulse facilitation is known to have an NMDA-mediated component [7]. It might well be that the elevated excitation of NMDA receptors is also involved in these processes. This appears more than probable, considering that the glutamate concentration rises both in the core and in the peri-infarct region in focal ischaemia [10].

In our experiments, disinhibition induced by previous focal ischaemia could be further enhanced by n7X. This suggests that the cortical disinhibition capacity is not fully utilized after focal ischaemia, and/or the mechanisms of these two processes are at least partly different.

Whatever the mechanisms, alterations in excitability in extensive cortical regions may have a significant impact on the ability of the function in the cerebral cortex to be reorganized following peripheral or central injury.

Acknowledgements

This work was supported by grants from NATO (LST.CLG.976235), NKFP 1/027 and from OTKA (T031893, M36213 and F37407). T.F. and Z.K. received a Békésy György postdoctoral fellowship (BÖ 211/2001 and BÖ 163/2002).

References

[1] I. Buchkremer-Ratzmann, O.W. Witte, Extended brain disinhibition following small photothrombotic lesions in rat frontal cortex, NeuroReport 8 (1997) 519–522.
[2] M.B. Calford, Dynamic representational plasticity in sensory cortex, Neuroscience 111 (2002) 709–738.
[3] D. Centonze, E. Saulle, A. Pisani, G. Bernardi, P. Calabresi, Adenosine-mediated inhibition of striatal GABAergic synaptic transmission during in vitro ischemia, Brain 124 (2001) 1855–1865.
[4] R.A. Diesz, D.A. Prince, Frequency-dependent depression of inhibition in guinea-pig neocortex in vitro by GABAB receptor feed-back on GABA release, J. Physiol. 412 (1989) 513–541.
[5] T. Farkas, J. Perge, Z. Kis, J.R. Wolff, J. Toldi, Facial nerve injury-induced disinhibition in the primary motor cortices of both hemispheres, Eur. J. Neurosci. 12 (2000) 2190–2194.
[6] F. Gallyas, J.R. Wolff, H. Böttcher, L. Záborszky, A reliable method for demonstrating axonal degeneration shortly after axotomy, Stain Technol. 55 (1980) 291–297.
[7] R.M. Joy, T.E. Albertson, NMDA receptors have a dominant role in population spike-paired pulse facilitation in the dentate gyrus of urethane-anesthetized rats, Brain Res. 604 (1993) 273–282.
[8] G. Meis, T. Iijima, K.A. Hossmann, Correlation between peri-infarct DC shifts and ischemic neuronal damage in rat, NeuroReport 6 (1993) 709–711.
[9] T. Mittmann, H.J. Luhmann, R. Schmidt-Kastner, U.T. Eysel, H. Weigel, U. Heinemann, Lesion-induced transient suppression of inhibitory function in rat neocortex in vitro, Neuroscience 60 (1994) 891–906.
[10] T. Morimoto, M.Y. Globus, R. Busto, E. Martinez, M.D. Ginsberg, Simultaneous measurement of salicylate hydroxylation and glutamate release in the penumbral cortex following transient middle cerebral artery occlusion in rats, J. Cereb. Blood Flow Metab. 16 (1996) 92–99.
[11] J. Nabekura, T. Ueno, A. Okabe, A. Furuta, T. Iwaki, C. Shimizu-Okabe, A. Fukuda, N. Akaike, Reduction of KCC2 expression and GABAA receptor-mediated excitation after in vivo axonal injury, J. Neurosci. 22 (2002) 4412–4417.
[12] T. Neumann-Haefelin, J.F. Staigner, C. Redecker, K. Zilles, J.M. Fritschy, H. Mohler, O.W. Witte, Immunohistochemical evidence for dysregulation of the GABAergic system ipsilateral to photochemically induced cortical infarcts in rats, Neuroscience 87 (1998) 871–879.
[13] J.N. Sanes, J.P. Donoghue, Plasticity and primary motor cortex, Annu. Rev. Neurosci. 23 (2000) 393–415.
[14] K. Schiene, J.F. Staiger, C. Bruehl, O.W. Witte, Enlargement of cortical vibrissa representation in the surround of an ischemic cortical lesion, J. Neurol. Sci. 162 (1999) 6–13.
[15] J. Toldi, T. Farkas, J. Perge, J.R. Wolff, Facial nerve injury produces a latent somatosensory input through recruitment of the motor cortex in the rat, NeuroReport 10 (1999) 2143–2147.
[16] J. Toldi, R. Laskawi, M. Landgrebe, J.R. Wolff, Biphasic reorganisation of somatotopy in the primary motor cortex follows facial nerve lesions in adult rats, Neurosci. Lett. 203 (1996) 179–182.
[17] A.N. van den Pol, K. Obrietan, G. Chen, Excitatory actions of GABA after neuronal trauma, J. Neurosci. 16 (1996) 4283–4292.

European Journal of Neuroscience, Vol. 15, pp. 937–943, 2002

SHORT COMMUNICATION
Oestrogen-dependent tracing in the rat CNS after pseudorabies virus infection

Szatmár Horváth,[1] Zsolt Kis,[1] Zsolt Boldogköi,[2] Antal Nógrádi[3] and József Toldi[1]
[1]Department of Comparative Physiology, University of Szeged, H-6701 Szeged, POB 533, Hungary
[2]Neurobiology Research Group, Department of Anatomy, Semmelweis University Medical School, H-1094 Budapest, Hungary
[3]Neuromorphology Laboratory, Department of Ophthalmology, University of Szeged, Faculty of General Medicine, H-6720 Szeged, Hungary

Abstract

This study examines the hypothesis that neuronal infectivity and the spreading of the pseudorabies virus (PRV) through the synapses in the central nervous system (CNS) are influenced by the oestrogen levels. The arcuate nucleus (ARC) and the subfornical organ (SFO) were chosen as models for analysis; the neurons in both structures possess oestrogen receptors and are mutually connected. A genetically engineered pseudorabies virus (Ba-DupLac) was used as a transneuronal tract tracer. This virus is taken up preferably by axon terminals, and transported very specifically through the synapses in a retrograde manner. Ba-DupLac was injected into the ARC of rats, followed by monitoring of the PRV-immunoreactivity (PRV-IR) in the SFO 72 h following inoculation. We found no PRV immunolabelling in the SFO of ovariectomized (OVX) rats, or in those OVX animals that received oestrogen shortly (4 h) before PRV infection (OVX + E 4 h). In contrast, in those OVX animals that received oestrogen 12 h before PRV infection (OVX + E 12 h), and also in intact control animals, PRV-IR was demonstrated in the SFO in all cases. Surprisingly, a reverse labelling was observed in the OVX rats; PRV-IR appeared in the pyriform cortex, whereas PRV-IR could not be detected in the control and OVX + E 12 h animals. As far as we are aware, this is the first study to demonstrate that transneuronal PRV labelling depends on the effects of oestrogen on certain CNS structures and connections.

Keywords: arcuate nucleus, neuronal plasticity, pseudorabies virus, subfornical organ

Introduction

In the past decade, a number of publications have demonstrated that oestrogen induces plastic alterations in the synaptic connections in the central nervous system (CNS) (Perez *et al.*, 1990; Párducz *et al.*, 1993; Frankfurt, 1994; Langub *et al.*, 1994; Leedom *et al.*, 1994; Naftolin *et al.*, 1996; VanderHorst & Holstege, 1997). Frankfurt *et al.* (1990) reported an increased density of dendritic spines and axodendritic synapses in the ventromedial hypothalamus after oestrogen exposure. A similar phenomenon was observed in the hippocampus (Woolley, 1998), whereas Naftolin *et al.* (1996) detected a reduced number of synaptic contacts in the arcuate nucleus (ARC) on the morning of estrus.

Recent studies have shown that pseudorabies virus (PRV) inoculation into the oestrogen-dependent organs (e.g. the uterine cervix) results in the widespread PRV infection of CNS structures (Lee & Erskine, 2000; Weiss *et al.* 2001).

To test whether oestrogen really does influence the susceptibility of CNS structures to PRV infection, we examined the oestrogen-dependent spread of PRV infection between the neurons of the ARC and the subfornical organ (SFO), the neurons of both of which possess oestrogen receptors (Shughrue *et al.*, 1997). The hypothalamic ARC is known to play an important role not only in the neuroendocrine function (Sawyer, 1979) but also in the control of the cardiovascular system (O'Neil & Brody, 1985; Brody *et al.*, 1986; Mastrianni *et al.*, 1989; Kunos *et al.*, 1991). The SFO, one of the circumventricular organs, is involved in the mechanisms controlling thirst, the salt–water balance, the arterial pressure, the plasma osmolarity (Robertson *et al.*, 1983; Gutman *et al.*, 1988; Ciriello & Gutman, 1991) and gonadotropin secretion (Limonta *et al.*, 1981). Anatomical studies have revealed that the SFO and the ARC are mutually connected; the SFO projects directly to the ARC (Gruber *et al.*, 1987), and the ARC sends efferents to the SFO (Rosas-Arellano & Ciriello, 1992).

These observations, taken together with the electrophysiological finding that the ARC neurons exert different effects (inhibition or excitation) on subpopulations of neurons in the SFO (Rosas-Arellano *et al.*, 1993), suggest the possibility of a feedback loop by which the ARC may influence the excitability of the SFO output neurons in response to bloodborne substances. In addition, the SFO may alter the sensitivity of the ARC neurons to incoming afferent inputs (Gruber *et al.*, 1987).

Male, female and ovariectomized (OVX) female rats treated with oestrogen (OVX + E) or untreated (OVX) were studied. A PRV was utilized as a transneuronal tract-tracing tool. The major advantage of herpesviruses over traditional transynaptic tracers is that they can self-amplify after crossing synapses (Card *et al.*, 1993). The transport

Correspondence: Dr J. Toldi, as above.
E-mail: toldi@bio.u-szeged.hu

Received 9 March 2001, revised 3 January 2002, accepted 21 January 2002

TABLE 1. Summary of data from the 5 groups of rats given PRV injections

	Numbers of labelled neurons				
	Vehicle treatment			Oestrogen treatment	
Brain area*	Intact males (n = 6)	Intact females (n =7)	OVX females (n =4)	OVX + E 4 h (n =4)	OVX + E 12 h (n =4)
Ipsilateral ARC	66.0 ± 4.1	74.5 ± 7.7	76.3 ± 8.9	73.7 ± 4.5	68.5 ± 5.4
Contralateral ARC	34.8 ± 5.2	39.5 ± 3.5	38.8 ± 5.1	40.6 ± 1.7	36.9 ± 7.2
Ipsilateral SFO	4.4 ± 0.3	6.9 ± 2.4	0	0	3.1 ± 0.6
Contralateral SFO	1.6 ± 0.5	2.9 ± 1.3	0	0	1.2 ± 0.5

*Ipsilateral/contralateral to injection site. Numbers of labelled neurons are given as means ± SD. OVX + E 4 h/12 h, ovariectomized females that received a single dose of 17β-estradiol 4 h/12 h before PRV injections. Sesame oil was used as vehicle.

of an attenuated PRV variant, strain Bartha (PRV-Ba) (Bartha, 1961), between CNS neurons has been reported to occur predominantly at points of synaptic contact, and to proceed in the retrograde direction, i.e. from axon terminals through the cell body to the presynaptic afferents (for a review, see Enquist *et al.*, 1998). We used Ba-DupLac, a genetically modified PRV-Ba derivative that was developed for tract-tracing studies.

Materials and methods

Animals and surgical procedures

The experimental procedures used in this study followed the protocol for animal care approved by the Hungarian Health Committee (1998) and by the European Communities Council Directives (86/609/EEC). All efforts were made to minimize the number of animals used. A total of 28 adult Sprague-Dawley rats (22 females and six males) were raised with access to water and food pellets (Altromin) *ad libitum*. Fourteen of the 22 females were ovariectomized (OVX) by means of bilateral dorsal incisions. All the surgical procedures were carried out under deep ketamine/xylazine anaesthesia (ketamine 10.0 mg/100 g and xylazine 0.8 mg/100 g body weight, i.p.). Eight females and six males remained intact. Vaginal smears were taken daily from the control females throughout at least two consecutive 4-day oestrus cycles before PRV injection.

Fourteen days after OVX, the operated female rats (n = 14) were divided into three groups: (i) those (n = 4) that received a single dose of 17β-estradiol (100 μg/100 g in sesame oil, i.p.) 4 h before PRV injection (OVX + E 4 h); (ii) those (n = 4) that received a single dose of 17β-estradiol (100 μg/100 g in sesame oil, i.p.) 12 h before PRV injection (OVX + E 12 h); and (iii), those (n = 6) that received an injection of vehicle alone (OVX). Intact males and females received an injection of vehicle 4 or 12 h before PRV injection. In three of the 28 animals, the PRV infection was not successful; PRV-IR neurons were not found in the ARC. In this study, only those animals in which the result of inoculation was positive were evaluated (n = 25). The data on the groups involved in this study are detailed in Table 1.

Cells and virus

A porcine kidney cell line, PK-15, was used for the propagation and titration of PRV. Cells were grown in Dulbecco's modified minimum essential medium (DMEM) supplemented with 5% foetal calf serum at 37 °C in a CO_2 incubator. Aliquots of PRV (1000 μL *per* vial) were stored at –80 °C, and single vials were thawed immediately prior to injection.

Construction of the recombinant virus

The *Bam*HI-8′fragment of PRV was isolated from the gel, and subcloned to pRL525, a palindrome containing a positive-selection vector (Elhai & Wolk, 1988). The targeting plasmid (pB8′Dra-Lac) was constructed by insertion of the lacZ-expression cassette to the unique *Dra*I recognition site of the *Bam*HI-8′ fragment in multiple steps. The general structure of the *lacZ* gene cassette was as follows. The reporter gene was controlled by the human cytomegalovirus immediate early 1 promoter/enhancer, and terminated by the simian virus 40 polyadenylation/termination (polyA) sequence. Recombinant virus was generated by the cotransfection of actively growing PK-15 cells with the purified PRV-Ba DNA and pB8′Dra-Lac via electroporation, as recently described (Boldogköi *et al.*, 2000). LacZ-containing virus was screened by means of the appearance of blue plaques in the presence of X-Gal, the chromogenic substrate of β-Gal. The plaques were selectedand plaque-purified to homogeneity through 3–5 rounds of purification steps.

Injection of the virus

Fourteen days after OVX, the animals were reanaesthetized. The head of each rat was fixed in a stereotactic headholder (David Kopf), onto which a special Hamilton syringe (tip outer diameter 200 μm) was mounted. The PRV was injected with special care; the inoculations were carried out by the same person at the following coordinates: frontal, –2.5 mm (to the bregma); lateral, 0.2 mm; vertical, 9.0 mm from the cortical surface (Paxinos & Watson, 1998). The injection of 0.1 μL PRV was achieved over 5 min by pressure (PRV concentration 10^9 pfu/mL; vehicle, DMEM + 5% foetal calf serum). After completion of the injection, the pipette remained in the tissue for an additional 5 min in order to prevent any backflow of the PRV or its spread into the surrounding areas. After the PRV injection, the incision on the head was closed and each animal was housed individually in a plastic isolation cage. The necessary precautions relating to the handling of PRV were taken throughout the experiment. All materials that came into contact with PRV during surgery were cleaned in 95% ethanol and Softa-Man solution and disposed of as biohazardous materials. The presence and location of PRV-IR neurons were checked in all animals. Of the 28 animals injected in these experiments, 25 (89%) were subsequently observed to have PRV-IR neurons in the ARC at the time of death (72 h after PRV infection). The positions of the tip of the Hamilton syringe and the lesion induced by the PRV injection were verified histologically in cresyl violet-stained sections. Only those animals were evaluated (n = 25) in which the infection was successful, i.e. primary infected neurons (PRV-IR) were seen in the ARC, and the terminal part of the penetration channel was localized exactly in the ARC.

Perfusion and immunocytochemistry

After survival for 72 h, animals were deeply anaesthetized with a mixture of Ketavet/Rompun solution as described above and perfused transcardially with approximately 200 mL of phosphate-buffered saline (PBS, 0.1 mol/L, pH 7.3), followed by approximately 200 mL of Zamboni's fixative. Brains were postfixed in fresh Zamboni's solution overnight. Coronal sections of the brain (50 μm) were obtained using a vibratome (Campden Instruments) and every fifth section was processed for PRV immunocytochemistry.

The sections were blocked in 5% normal goat serum (diluted in PBS) for 1 h, and incubated with a rabbit polyclonal antibody (Rb133; 1 : 10 000, courtesy of Professor L. W. Enquist, Department of Molecular Biology, Princeton University, Princeton, USA) overnight at 4 °C. The sections were then treated with biotinylated anti-rabbit IgG (1 : 200, Vector Laboratories) for 2 h at room temperature. The immunohistochemical reaction was visualized with the ABC–DAB technique; sections were mounted on gelatinized slides, dehydrated and coverslipped with Entellan® (Fluka). Sections containing labelled cells in the ARC or SFO were included in cell counting. As every fifth section was processed for PRV immunohistochemistry, four sections were used in both the ARC and SFO in each animal, and all the positive neurons were counted in these structures.

Statistical analysis

Statistical analysis was performed with the aid of the SPSS 9.0 for Windows program. The results are expressed as means ± standard deviation (SD). The significance of differences in the data was determined by one-way analysis of variance (ANOVA), followed by Bonferoni's *post hoc* analysis. A P-value less than 0.05 was regarded as significant.

Results

PRV immunoreactivity in intact females and males

Efforts were made to determine the exact phase of the oestrus cycle in females. As we could not precisely determine this, we used a larger number of intact females for inoculation with PRV.

In these animals, primary infected neurons were found in the ARC, around the end of the penetration channel. In all the evaluated intact animals, PRV-IR neurons were also seen in the SFO (Table 1 and Fig. 1A–D). The specificity of PRV injection is shown by the lateralization; a higher number of labelled neurons were found on the injected (left) side (males 66.0 ± 4.1; females 74.5 ± 7.7 labelled neurons) than on the contralateral side (males 34.8 ± 5.2; females 39.5 ± 3.5; see Fig. 1A and B and Table 1). In the ARC, no significant differences were found between male and female control animals.

PRV-IR neurons were also found in the SFO of both males and females. Significant differences were observed between females and males in the number of infected SFO neurons (males 4.4 ± 0.3; females 6.9 ± 2.4 on the injected side; see Table 1).

Labelled neurons were rarely found in other hypothalamic structures, and were therefore not studied systematically elsewhere.

PRV immunoreactivity in ovariectomized animals

In the OVX animals treated with vehicle, PRV-IR neurons were found only in the ARC, as a result of the primary infection (similar to Fig. 1A and B and Table 1), but not in the SFO. These primary infected cells displayed cytoplasmic staining and, by 72 h following infection, various intensities of PRV-IR could be seen in these neurons. The number of labelled neurons in the ARC of the OVX animals did not change significantly as compared to the intact females (Fig. 2).

Careful observation of sections derived from the brains of the OVX rats revealed no sign of PRV-IR in the SFO (Table 1 and Fig. 3A), but PRV-IR neurons appeared in the pyriform cortex in all of these animals (Fig. 3C). It was interesting that PRV-IR was observed in the pyriform cortex in the OVX rats, whereas staining was not seen at all in the SFO of these animals. However, in the controls and the OVX + E 12 h animals, which exhibited stained neurons in the SFO (see details below), PRV-IR was found in the pyriform cortex in only a single neuron of one animal (not shown).

PRV-IR in oestradiol-treated ovariectomized rats

In these animals, primarily infected neurons were found in the immediate vicinity of the penetration channel in the ARC, as described above.

In the SFO of the OVX + E animals, however, PRV-IR neurons were observed in only one of the two groups. The animals which were treated with 17β-estradiol 4 h before inoculation (OVX + E 4 h group) did not exhibit PRV-positive neurons in their SFO (similarly as shown in Fig. 3A). However, all the animals in the OVX + E 12 h group contained PRV-IR in the neurons in the SFO (Table 1 and Fig. 3B). These PRV-infected cells displayed strong cytoplasmatic staining (as in Fig. 1C, inset). The lateralization in labelling could also be seen in the SFO, i.e. there was either only staining ipsilateral to the inoculation (Fig. 3B) or a higher number of labelled cells were found on the ipsilateral side: 3.1 ± 0.6 on the injected side and 1.2 ± 0.5 on the control side (as in Fig. 1C and D and Table 1).

The statistical analysis did not reveal a significant difference in the ARC between the groups, either ipsilateral to the inoculation ($F_{4,20} = 1.267$, $P = 0.316$) or contralateral to it ($F_{4,20} = 2.383$, $P = 0.086$, see Table 1 and Fig. 2). In the SFO, however, the groups differed significantly both ipsilateral to the inoculation ($F_{2,14} = 8.07$, $P = 0.005$) and contralateral to it ($F_{2,14} = 5.1$, $P = 0.0022$). Bonferroni's *post hoc* test showed that there was not a significant difference in the number of labelled cells in the SFO between the OVX + E 12 h animals and the intact males. The numbers of labelled neurons in these groups, however, were much lower than in the intact females.

The numbers of labelled neurons both ipsilateral and contralateral to the inoculation in the groups of females differ significantly from those found on the respective sides of the other groups (see Fig. 4).

Discussion

The present study has demonstrated an oestrogen-dependent transneuronal spread of PRV from the ARC to the SFO and pyriform cortex of female rats. The main observations were as follows: in the presence of oestrogen (intact and OVX + E 12 h animals), PRV was transported from the primarily infected neurons in the ARC to the SFO, but not to the pyriform cortex (with the exception of a single neuron labelled in one animal). By contrast, in the absence of oestrogen or before the oestrogen had had time to exert its effect (OVX and OVX + E 4 h animals), we never observed PRV infection in the SFO cells following ARC inoculation, whereas strongly labelled neurons appeared in the pyriform cortex of these animals. The reverse labelling of the pyriform cortex, rather than that of the SFO, is surprising, and we have no definite explanation for this phenomenon at present. We could not observe a correlation between the labelling (in the SFO vs. the pyriform cortex) and the phases of

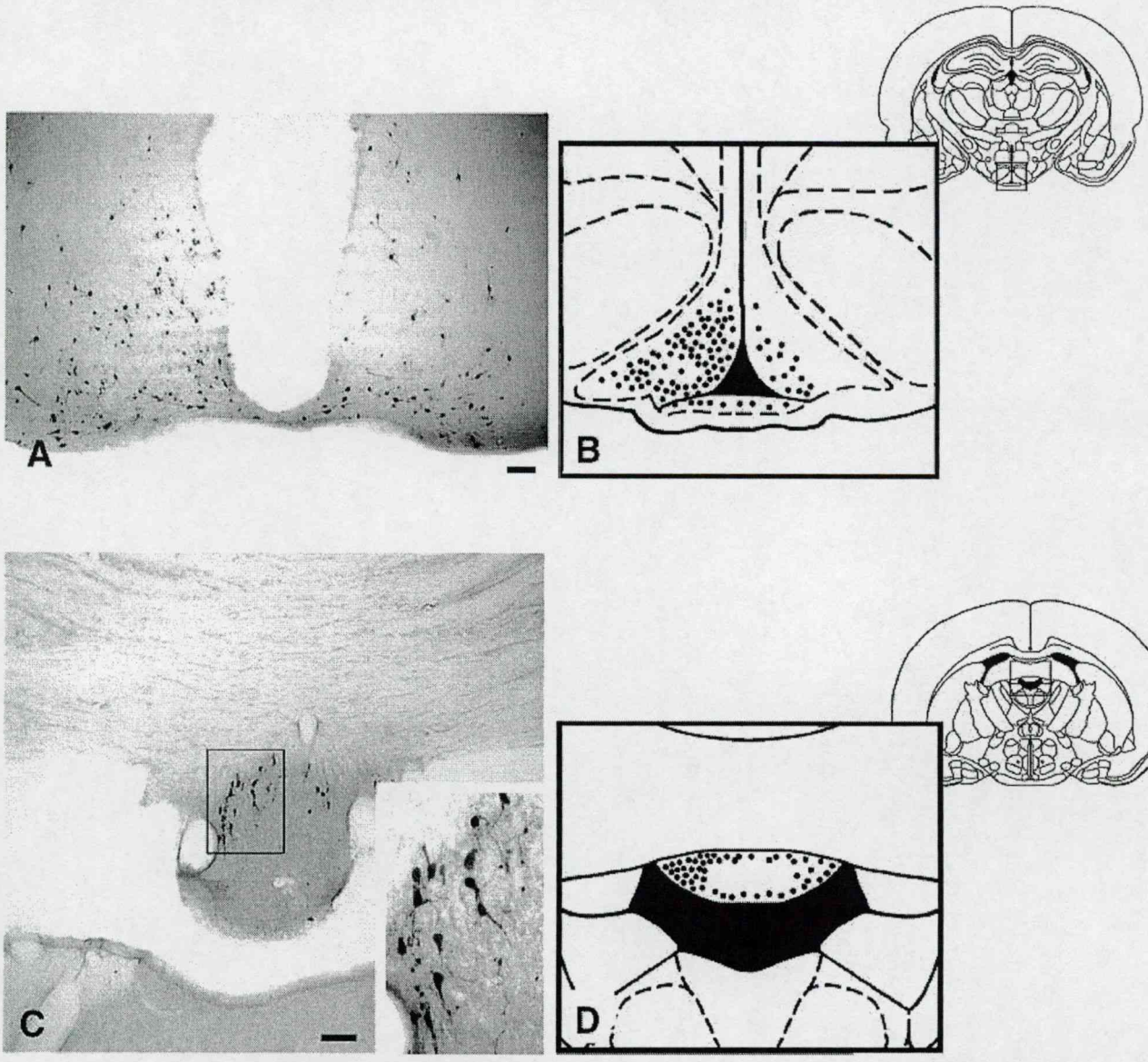

FIG. 1. Primarily infected neurons in the arcuate nucleus (ARC) 72 h after the injection of PRV into the nucleus in a control animal. (A) Labelled neurons in the medial posterior part of the arcuate hypothalamic nucleus (ARC), at low magnification. Note the specificity of the PRV injection and the higher number of labelled neurons on the injected side (left). (B) Number and localization of immunoreactive neurons in the ARC are indicated, using a drawing modified after Paxinos & Watson (1998). Each dot represents one neuron; the total number of neurons labelled in this Figure indicates the total number of labelled neurons in one animal. The boxed area in the schematic diagram (top right-hand corner of panel B) shows the enlarged area in B. (C and D) Secondary infected neurons in the SFO following the injection of PRV into the ARC of an intact animal. The boxed area in C is shown at higher magnification in the bottom right-hand corner of panel C. The boxed area in the schematic diagram (top right-hand corner of panel D) shows the enlarged area in D, in which the number and localization of the immunoreactive neurons in the SFO of one animal are indicated, using a drawing modified after Paxinos & Watson (1998). Note the higher number of labelled neurons on the injected side (left). Scale bar, 100 μm.

the oestrus cycle. Although we made efforts to determine the distinct phases of cycle, we did not observe the cycling clearly in each case. Therefore, we argue that although the females were in different phases (e.g. in oestrus or pro-oestrus) of their cycle, the methods we use did not allow an exact evaluation of the cycle. Because of this uncertainty, we used more control females than the number of animals in the OVX groups (seven animals vs. four animals, respectively). The hormonal influence of the different phases of the oestrus cycle in the intact females used in this study was reflected by the relatively high standard deviation for the number of labelled cells. These results, which are supported by the statistical analysis, suggest that relatively low levels of oestrogen are able to produce labelling in the SFO both in males (due to the activity of the enzyme aromatase) and in females (independently of the actual phase of the oestrus cycle). However, this was not the case in the OVX and OVX + E 4 h animals, where the oestrogen levels were likely to be so critically low as not to produce labelling. Zhu & Pfaff (1998) reported that a relatively short length of time (60 min) was sufficient to induce

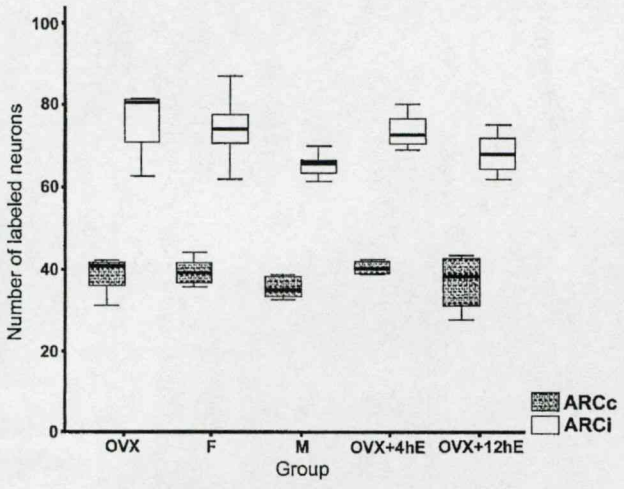

FIG. 2. The diagram shows the number of labelled neurons in the ARC of the different animal groups. OVX, ovariectomized animals; F, females; M, males; OVX + E 4 h, 17β-estradiol treatment 4 h before virus injection; OVX + E 12 h, 17β-estradiol treatment 12 h before virus injection; ARCi, arcuate nucleus ipsilateral to the inoculation; ARCc, arcuate nucleus contralateral to the inoculation. Median values are presented by transverse lines. Boxes relate to a probability of 95%. There is no significant difference in the number of labelled neurons between the groups, neither ipsilateral nor contralateral to the inoculation.

changes in the binding of an AP-1 nuclear transcription factor (such as c-fos or c-jun) in the rat hypothalamus after oestrogen application. Nuclear ultrastructural changes were observed in the hypothalamic neurons 2 h after oestrogen treatment in OVX animals (Jones *et al.*, 1985). In our experiments, however, no transneuronal labelling was produced 4 h after oestrogen application. These findings suggest that the oestrogen dependence of PRV labelling is based on long-latency changes involving gene expression rather than on transcriptional mechanisms.

As far as we know, the present study is the first to demonstrate oestrogen-dependent tracing with PRV in the CNS. Our working hypothesis is based on the assumption that, by selecting a PRV strain with a highly attenuated phenotype and specific spreading characteristics, we can create a system based on the 'all or none' principle, i.e. transneuronal PRV labelling does not work below a critical level of oestrogen.

The results of this study suggest that, in the absence of oestrogen, the connections between the ARC and the SFO do not permit the transmission of PRV to the SFO, but this situation is altered in the presence of oestrogen. This oestrogen-dependent labelling of the SFO could possibly be induced by the oestrogen-dependent synaptic plasticity, which has been well documented in several regions of the CNS (Chung *et al.*, 1988; Párducz *et al.*, 1993; Langub *et al.*, 1994; Naftolin *et al.*, 1996; VanderHorst & Holstege, 1997; Woolley, 1998; Flanagan-Cato *et al.*, 2001).

However, if oestrogen plays a key role in the regulation of synaptic remodelling in some brain structures, then the action of oestrogen on oestrogen-sensitive neurons within these areas might be expected to influence both the incidence and the rate of PRV infectivity by altering the synaptic connections between these structures.

It is well established that neurons in the SFO send axons directly to the ARC (Gruber *et al.*, 1987). The anatomical data and our own results suggest that the existence of the synaptic contacts between the axon terminals of the neurons in the SFO and the ARC neurons is

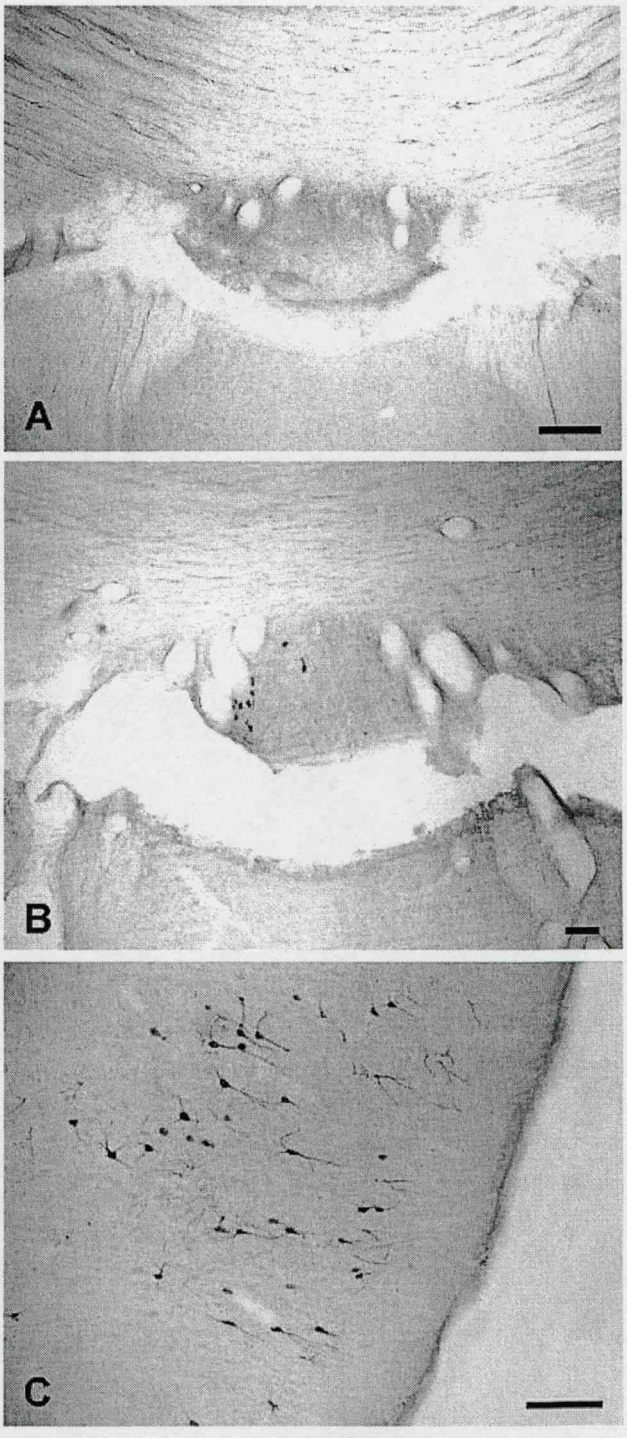

FIG. 3. (A) Lack of secondarily infected PRV-immunoreactive neurons in the SFO of an ovariectomized (OVX) animal. Note the complete lack of staining 72 h after PRV inoculation. Scale bar, 100 μm. (B) Immunoreactive neurons in the SFO of an OVX animal which received estradiol 12 h before virus infection (OVX + E 12 h). Note the presence of PRV-immunoreactive cells in the SFO. Scale bar, 100 μm. (C) PRV-immunoreactive neurons in the pyriform cortex of an OVX animal. Scale bar, 100 μm.

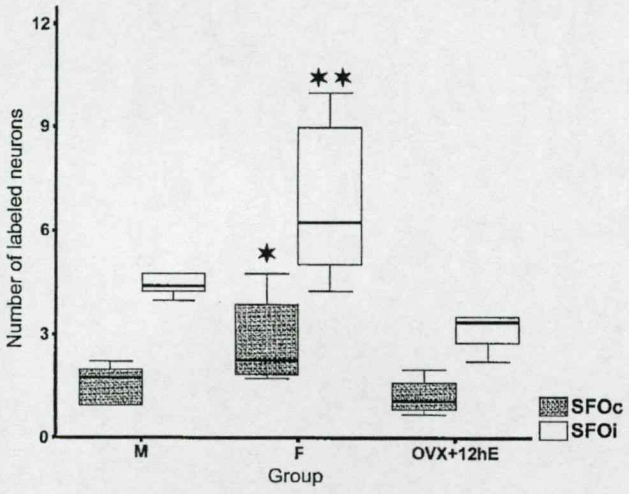

FIG. 4. The number of labelled neurons in the SFO of the different groups. SFOi, subfornical organ ipsilateral to the inoculation; SFOc, subfornical organ contralateral to the inoculation. All labels are as in Fig. 2. The numbers of labelled neurons both ipsilateral (**) and contralateral (*) to the inoculation in the groups of females differ significantly from those found on the respective sides of the other groups. Note the high variability in the number of labelled neurons in the group of females. The reason for this is probably that the animals were in different phase of the oestrus cycle.

oestrogen-dependent. Other studies have demonstrated that the densities of dendritic spines and axodendritic synapses in the hypothalamus (Frankfurt *et al.*, 1990) and in the hippocampus (Woolley, 1998) are oestrogen-dependent. An increase in the number of synaptic contacts between the supraspinal presynaptic neurons located in the nucleus retroambiguus of the caudal medulla and the spinal postsynaptic lumbar motoneurons in cats in estrus and in oestrogen-treated cats has been reported by VanderHorst & Holstege (1997). However, as reported by Naftolin *et al.* (1996), there are a reduced number of synaptic contacts between the cells in the ARC on the morning of oestrus. Párducz *et al.* (1993) found that this reduction was mainly due to a decrease in the number of γ-aminobutyric acid (GABA)ergic synapses, whereas the number of non-GABAergic axosomatic synapses did not change significantly.

Taken all together, as the number of synaptic connections between the ARC and the SFO is reversely influenced by oestrogen, this mechanism cannot provide a direct explanation for the increased labelling by PRV due to oestrogen treatment.

A second, more viable mechanism that could underlie the phenomenon is that oestrogen modulates the infectivity of neurons. Weiss *et al.* (2001) found that PRV injections into either the uterine cervix or the kidney produced an oestrogen-dependent infection in specific CNS structures. The oestrogen-dependence of transneuronal viral tracing from the kidney suggests that oestrogen influences the spread of PRV between CNS structures and not the uptake of virus from the site of injection. By contrast, Lee & Erskine (2000) found that PRV infectivity was not altered by oestrogen treatment. The reason for that result might be that they applied the PRV peripherally (uterine cervix) and not into the CNS. The different labelling patterns in the SFO and pyriform cortex lead us to suggest that the different types of neurons (different structures in the CNS) may be susceptible to virus infections in different ways, thereby resulting in the occurrence or lack of transneuronal viral labelling.

The results could also suggest that not only did the direct injection of PRV into the ARC infect the ARC neurons and then, by transneuronal spreading of the virus, the SFO neurons, but the terminals of the SFO neurons could have taken up the virus and also become primarily infected. Although this possibility cannot be excluded, the high number of primary infected ARC neurons suggest that neurons in the SFO were mainly infected by transneuronal spread of the virus.

These data and our own observations indicate that transneuronal PRV labelling depends on the effects of oestrogen on the CNS structures and connections, and that synaptic remodelling influenced by oestrogen is less likely to play a key role in the spread of PRV within the CNS.

Though little is known of the relation between the oestrogen receptors (ER-α and ER-β) and the oestrogen-dependent synaptic plasticity or neuronal infectivity, this is presumably also an important factor. From this point of view, it might be interesting that different types of ERs are expressed on the neurons in these structures, e.g. only ER-α was found in the SFO, whereas both ER-α and ER-β exist in the ARC (Shughrue *et al*, 1997).

These results demonstrate that PRV tracing is a suitable method for the evaluation of oestrogen-dependent labelling in the CNS.

Acknowledgements

The authors thank Prof. L. W. Enquist (Princeton University) for the gift of the primary antiserum. The research was supported by a grant from Higher Education and Research Development (FKFP 1195/1997) and by grants from the National Research Foundation (OTKA T031893 and M36213).

Abbreviations

ARC, arcuate nucleus; CNS, central nervous system; DMEM, Dulbecco's modified minimum essential medium; ER, oestrogen receptor; F, female rat; GABA, γ-aminobutyric acid; OVX, ovariectomized female rat; OVX, + E 4 h ,ovariectomized female rat treated with oestrogen 4 h before PRV infection; OVX + E 12 h, ovariectomized female rat treated with oestrogen 12 h before PRV infection; M, male rat; PBS, phosphate-buffered saline; PRV, pseudorabies virus; PRV-IR, pseudorabies virus immunoreactivity; PRV-Ba, pseudorabies virus strain Bartha; SFO, subfornical organ.

References

Bartha, A. (1961) Experiments to reduce the virulence of Aujeszky's disease virus [in Hungarian]. *Magyar Állatorv. Lapj.*, **16**, 42–45.

Boldogköi, Z., Erdelyi, F. & Fodor, I. (2000) A putative latency promoter/enhancer (P (LAT2) region of pseudorabies virus contains a virulence determinant. *J. Gen. Virol.*, **81**, 415–420.

Brody, M.J., O'Neil, T.P. & Porter, J.P. (1986) Role of paraventricular and arcuate nuclei in cardiovascular regulation. In Magro, A., Osswald, W., Reis, D. & Vanhoutte, P. (eds), *Central and Peripheral Mechanisms of Cardiovascular Regulation*. Plenum, New York, pp. 443–464.

Card, J.P., Rinaman, L., Lynn, R.B., Lee, B.H., Meade, R.P., Miselis, R.R. & Enquist, L.W. (1993) Pseudorabies virus infection of the rat central nervous system: ultrastructural characterization of viral replication, transport, and pathogenesis. *J. Neurosci.*, **13**, 2515–2539.

Chung, S.K., Pfaff, D.W. & Cohen, R.S. (1988) Estrogen-induced alterations in synaptic morphology in the midbrain central gray. *Exp. Brain Res.*, **69**, 522–530.

Ciriello, J. & Gutman, M.B. (1991) Functional identification of central pressor pathways originating in the subfornical organ. *Can. J. Physiol. Pharmacol.*, **69**, 1035–1045.

Elhai, J. & Wolk, C.P. (1988) A versatile class of positive-selection vectors based on the nonviability of palindrome-containing plasmids that allows cloning into long polylinkers. *Gene*, **68**, 119–138.

Enquist, L.W., Husak, P.J., Banfield, B.W. & Smith, G.A. (1998) Infection and

spread of alphaherpesviruses in the nervous system. *Adv. Virus Res.*, **51**, 237–347.

Flanagan-Cato, L.M., Calizo, L.H. & Daniels, D. (2001) The synaptic organization of vmh neurons that mediate the effects of estrogen on sexual behavior. *Horm. Behav.*, **40**, 178–182.

Frankfurt, M. (1994) Gonadal steroids and neuronal plasticity. Studies in the adult rat hypothalamus. *Ann. NY Acad. Sci.*, **743**, 45–59.

Frankfurt, M., Gould, E., Woolley, C.S. & McEwen, B.S. (1990) Gonadal steroids modify dendritic spine density in ventromedial hypothalamic neurons: a Golgi study in the adult rat. *Neuroendocrinology*, **51**, 530–535.

Gruber, K., McRae-Degueurce, A., Wilkin, L.D., Mitchell, L.D. & Johnson, A.K. (1987) Forebrain and brainstem afferents to the arcuate nucleus in the rat: potential pathways for the modulation of hypophyseal secretions. *Neurosci. Lett.*, **75**, 1–5.

Gutman, M.B., Ciriello, J. & Mogenson, G.J. (1988) Effects of plasma angiotensin II and hypernatremia on subfornical organ neurons. *Am. J. Physiol.*, **254**, 746–754.

Jones, K.J., Pfaff, D.W. & McEwen, B.S. (1985) Early estrogen-induced nuclear changes in rat hypothalamic ventromedial neurons: an ultrastructural and morphometric analysis. *J. Comp. Neurol.*, **239**, 255–266.

Kunos, G., Mastrianni, J.A., Moscqueda-Garcia, R. & Varga, K. (1991) Endorphinergic neurons in the brainstem: role in cardiovascular regulation. In Kunos, G. & Ciriello, J. (eds), *Central Neural Mechanism in Cardiovascular Regulation*. Birkhauser, Boston, pp. 122–136.

Langub, M.C.J., Maley, B.E. & Watson, R.E.J. (1994) Estrous cycle-associated axosomatic synaptic plasticity upon estrogen receptive neurons in the rat preoptic area. *Brain Res.*, **641**, 303–310.

Lee, J.W. & Erskine, M.S. (2000) Pseudorabies virus tracing of neural pathways between the uterine cervix and CNS: effects of survival time, estrogen treatment, rhizotomy, and pelvic nerve transection. *J. Comp. Neurol.*, **418**, 484–503.

Leedom, L., Lewis, C., Garcia-Segura, L.M. & Naftolin, F. (1994) Regulation of arcuate nucleus synaptology by estrogen. *Ann. NY Acad. Sci.*, **743**, 61–71.

Limonta, P., Maggi, R., Giudici, D., Martini, L. & Piva, F. (1981) Role of the subfornical organ (SFO) in the control of gonadotropin secretion. *Brain Res.*, **229**, 75–84.

Mastrianni, J.A., Palkovits, M. & Kunos, G. (1989) Activation of brainstem endorphinergic neurons causes cardiovascular depression and facilitates baroreflex bradycardia. *Neuroscience*, **33**, 559–566.

Naftolin, F., Mor, G., Horvath, T.L., Luquin, S., Fajer, A.B., Kohen, F. & Garcia-Segura, L.M. (1996) Synaptic remodeling in the arcuate nucleus during the estrous cycle is induced by estrogen and precedes the preovulatory gonadotropin surge. *Endocrinology*, **137**, 5576–5580.

O'Neil, T.P. & Brody, M.J. (1985) Hemodynamic effects produced by arcuate stimulation are mediated in part through a projection to paraventricular nucleus. *Fed. Proc. Abstr.*, **44**, 1553.

Párducz, A., Perez, J. & Garcia-Segura, L.M. (1993) Estradiol induces plasticity of gabaergic synapses in the hypothalamus. *Neuroscience*, **53**, 395–401.

Paxinos, G. & Watson, C. (1998) *The Rat Brain in Sterotaxic Coordinates*. Academic Press, Sydney.

Perez, J., Naftolin, F. & Garcia-Segura, L.M. (1990) Sexual differentiation of synaptic connectivity and neuronal plasma membrane in the arcuate nucleus of the rat hypothalamus. *Brain Res.*, **527**, 116–122.

Robertson, A., Kucharczyk, J. & Mogenson, G.J. (1983) Drinking behavior following electrical stimulation of the subfornical organ in the rat. *Brain Res.*, **274**, 197–200.

Rosas-Arellano, M.P. & Ciriello, J. (1992) Direct innervation of circumventricular organs by arcuate nucleus neurons. *Soc. Neurosci. Abstr.*, **18**, 1174.

Rosas-Arellano, M.P., Solano-Flores, L.P. & Ciriello, J. (1993) Effect of arcuate nucleus activation on neuronal activity in subfornical organ. *Brain Res.*, **619**, 352–356.

Sawyer, C.H. (1979) The seventh Stevenson Lecture. Brain amines and pituitary gonadotrophin secretion. *Can. J. Physiol. Pharmacol.*, **57**, 667–680.

Shughrue, P.J., Lane, M.V. & Merchenthaler, I. (1997) Comparative distribution of estrogen receptor-alpha and -beta mRNA in the rat central nervous system. *J. Comp. Neurol.*, **388**, 507–525.

VanderHorst, V.G. & Holstege, G. (1997) Estrogen induces axonal outgrowth in the nucleus retroambiguus-lumbosacral motoneuronal pathway in the adult female cat. *J. Neurosci.*, **17**, 1122–1136.

Weiss, M.L., Dobbs, M.E., MohanKumar, P.S., Chowdhury, S.I., Sawrey, K., Guevara-Guzman, R. & Huang, J. (2001) The estrous cycle affects pseudorabies virus (PRV) infection of the CNS. *Brain Res.*, **893**, 215–226.

Woolley, C.S. (1998) Estrogen-mediated structural and functional synaptic plasticity in the female rat hippocampus. *Horm. Behav.*, **34**, 140–148.

Zhu, Y.S. & Pfaff, D.W. (1998) Differential regulation of AP-1 DNA binding activity in rat hypothalamus and pituitary by estrogen. *Brain Res. Mol. Brain Res.*, **55**, 115–125.

Psychopharmacology (2002) 160:1–8
DOI 10.1007/s00213-001-0957-2

ORIGINAL INVESTIGATION

**Hajnalka Németh · Hedvig Varga · Tamás Farkas
Zsolt Kis · László Vécsei · Szatmár Horváth
Krisztina Boda · Joachim R. Wolff · József Toldi**

Long-term effects of neonatal MK-801 treatment on spatial learning and cortical plasticity in adult rats

Received: 24 September 2000 / Accepted: 7 October 2001 / Published online: 23 November 2001

Abstract *Rationale and objectives:* The long-term effects of neonatal treatment with MK-801 on spatial learning and cortical plasticity were investigated in adult rats. *Methods:* Rat pups were injected twice daily with MK-801 (0.1 mg/kg) on postnatal days 7–19, participated in water maze testing between postnatal days 90 and 102, and were then studied electrophysiologically. *Results:* Treatment with MK-801 in such a low dose resulted in a very slight impairment of performance in the water maze task, but not in the visual cue response. Besides the slight learning impairment, the electrophysiological study revealed a reduction in the capacity for plasticity in the primary motor cortex of the treated animals, which was pronounced in the controls. *Conclusion:* The study demonstrates that even a slight impairment in learning and memory function may be accompanied by a cortical plasticity deficiency that is detectable electrophysiologically.

Keywords Spatial learning · Water maze · MK-801 · NMDA receptor · Cortical plasticity · Evoked potential · Primary motor cortex · Disinhibition

H. Németh · H. Varga · T. Farkas · Z. Kis · S. Horváth · J. Toldi (✉)
Department of Comparative Physiology, University of Szeged,
POB 533, 6701 Szeged, Hungary
e-mail: toldi@bio.u-szeged.hu
Tel.: +36-62-544153, Fax: +36-62-544149

L. Vécsei
Department of Neurology, University of Szeged, POB 71,
6701 Szeged, Hungary

K. Boda
Department of Medical Informatics, University of Szeged,
Korányi fasor 9, 6720 Szeged, Hungary

J.R. Wolff
Department of Anatomy, University of Göttingen,
Kreuzbergring 36, 37075 Göttingen, Germany

Introduction

In the past decade, substantial evidence has accumulated that demonstrates a considerable degree of plasticity of the primary motor cortex (MI; see the recent review by Sanes and Donoghue 2000). Some plastic changes develop very rapidly. As an example, minutes after unilateral transection of the facial motoric nerve (N7x), the cortical responses evoked by trigeminal stimulation ipsilateral to the denervation are facilitated (both gross potentials and unit activity) in the MIs in both hemispheres (Toldi et al. 1999). Since these changes are not observed in control animals, but develop after facial nerve injury, and can be mimicked by picrotoxin, they are considered to be based on the disinhibition of pre-existing associative and commissural connections (Toldi et al. 1999; Farkas et al. 2000).

An increasing number of results suggest, however, that the transiently reduced inhibition (e.g. after nerve injury) is a necessary, but not sufficient condition for the development of MI plasticity. The potential for plasticity in the MI has been closely linked to the function of *N*-methyl-D-aspartate (NMDA) receptors (Qiu et al. 1990). Moreover, it has been shown that a component of field potentials itself evoked in the horizontal pathways of the rat motor cortex is mediated by NMDA receptors, and long-term potentiation (LTP) can develop in these horizontal connections (Hess and Donoghue 1994; Hess et al. 1994).

We recently reported that the MI responses evoked by contralateral trigeminal stimulation are conveyed mostly by horizontal associations from the primary somatosensory cortex (Farkas et al. 1999).

It therefore seems probable that the NMDA receptors play a decisive role in the responses in MI evoked by contralateral trigeminal stimulation, and especially in their potentiation.

NMDA receptors are additionally involved in higher brain functions: learning and memory. Their role in the acquisition of spatial memory tasks has also been extensively studied. It has been shown that neonatal treatment with MK-801 (a non-competitive NMDA receptor antag-

onist) results in the impairment of spatial learning in the adult rat (Gorter and de Bruin 1992).

The aim of this study was to test the hypothesis that even a minimal conflict with NMDA receptors in the early critical age of life, which results in mild if any detectable change in daily behaviour, induces hidden but life-long dysfunctions, which can be detected in different parts of the CNS with appropriate methods. Although spatial learning is attributed to one of the hippocampal functions, in the present study we intentionally tested the hypothesis in the motor cortex, which is probably not primarily involved in spatial learning, but the NMDA receptors play a decisive role in its processes. We presume that chronic neonatal MK-801 treatment, which results in only a mild if any impairment of spatial learning, further causes a detectable change (impairment) in the function of another brain structure, e.g. in cortical plasticity.

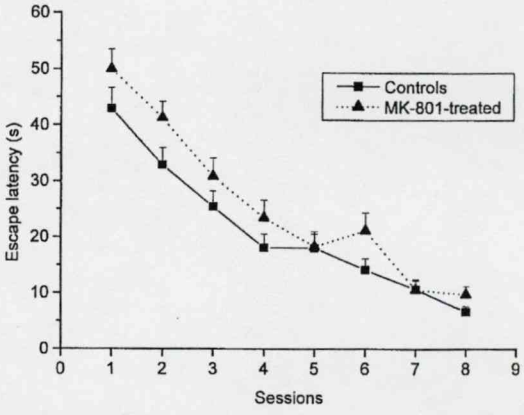

Fig. 1 Escape latencies (in seconds) of adult controls and MK-801-treated rats. Times (means±SE) needed to find the hidden platform during the eight sessions in experiment I. The performance of the MK-801-treated rats (0.1 mg/kg, twice daily, postnatal days 7–19) was slightly poorer than that of the saline-treated controls

Materials and methods

Animals

The experimental procedure used in this study followed the protocol for animal care approved by the Hungarian Health Committee (1998), the European Communities Council Directives (86/609/EEC) and the German Animal Protection Law (licence 509.425.02-99 to J.R.W.). Sprague-Dawley rats gave birth in our colony and the pups were randomly distributed among different mothers. Only male rats were used for this study. The treated animals (10 pups) received subcutaneous injections of 0.1 mg/kg MK-801 (dizocilpine; Sigma) twice daily, at 0900 and at 1700 hours, starting on postnatal day (PND) 7 and lasting until PND 19. The controls received an equal volume of saline vehicle (0.9% NaCl in sterile distilled water). The MK-801 treatment resulted in a body growth reduction, which more or less compensated after the treatment was stopped. The animals were weaned on PND 22 and were housed in large cages (four to six rats per cage). For the present study, 22 rats were used (MK-801-treated: n=10, controls: n=12). The animals were kept under 12-h light and 12-h dark conditions, with lights on at 0700 hours. The room temperature was 22±1°C. The rats were used for the water maze study between PNDs 90 and 102, and the electrophysiological study followed between PNDs 105 and 135.

Water maze

The rats were trained in a large circular swimming pool (165 cm in diameter, 0.7 m high) filled with water to a depth of 35 cm. The water was at room temperature and was made opaque by the addition of 3 l of milk. The pool was situated in a small rectangular room. The walls were equipped with a variety of spatial cues (a picture or a lamp giving diffused light), which remained unchanged during the experiment. A video camera was mounted above the centre of the pool. Animal movements were monitored, timed, and recorded on videotape. The pool was divided into four quadrants and a removable platform (8 cm in diameter) was hidden at any of four positions in the pool exactly 25 cm from the sidewall. The platform was 1.5 cm below the water surface and not visible to the swimming rat.

Experiment I (PNDs 90–97)

All animals were trained in five trials in each daily session. The intertrial interval was 30 s. For each rat, the platform location was fixed in a particular quadrant. The information about the localization of the platform was available to the rat exclusively from extra-maze cues. Within a session, the rats started each swim from different entry points. Each animal was placed into the pool facing the wall at one of the four entry points and was allowed a period of 60 s to escape to the platform. The escape latencies of each trial were measured. The animals were left on the platform for 20 s and then put into an empty cage for 30 s. If an animal failed to escape onto the platform within 60 s, it was placed there for 20 s, and was awarded a latency of 60 s for that trial. Means of latency of trials were calculated in each session (Fig. 1).

Experiment II (PNDs 101–102)

Following a 3-day interval, cue training was carried out on PNDs 101–102. This experiment was designed to allow an evaluation of the sensory and motoric capabilities. For non-spatial learning, a visible black platform (situated 1.5 cm above the surface of the water) was used as a visual cue. In each trial, the platform was positioned in any of the four possible quadrants in a random sequence. The rats were placed in the water, facing the wall, always at the same entry point.

Statistics

The effects of the treatment on the escape latencies in the water maze tasks and on the electrophysiological properties of the motor cortex were analysed by using repeated measures ANOVA (SPSS for Windows 9.0). For each animal, the escape latencies were used in the statistical analysis. The differences in body weights between the MK-801-treated animals and the controls were compared by using Student's t-test (mean±SD). A P level of <0.05 was used as a measure of significance in all statistical tests.

Electrophysiology

Surgical procedure

After the behavioural experiments, eight of the 12 controls and seven of the ten MK-801-treated animals participated in electrophysiological studies. During these experiments, the rats were anaesthetized with a mixture of Ketavet (10.0 mg/100 g) and Rompun (xylazine, 0.8 mg/100 g). On both sides, the MI was exposed by craniotomy from about 2 mm posterior to 5 mm anterior from the bregma, and from 0.5 to 5 mm lateral from the midline. In the

course of the operation, we also exposed the right side facial nerve, including its postauricular branch. This was transected later, during the electrophysiological recordings. After surgery, the animals were kept at rest for 1 h until the beginning of the recording sessions. The core temperature was maintained at 37±0.2°C.

Stimulation and recording

Electrical stimulation of the vibrissa pad or electromechanical vibrissa stimulation was employed to induce evoked potentials (EPs) in the MIs in both hemispheres. The details of stimulation and cortical recordings have been published elsewhere (Toldi et al. 1999; Farkas et al. 2000). In brief, the right whisker pad was stimulated electrically with bipolar needle electrodes (1 Hz, 0.3 ms duration, 150–200 μA) to evoke visible whisker movements. To investigate paired pulse inhibition effects on the amplitudes of EPs, a paired-pulse stimulation protocol was used (application of two electrical pulses with a 200 ms interstimulus interval). The ratio of the amplitudes of the EPs elicited by the second versus the first stimulus was calculated and defined as the Q-value (e.g. Q=EP2/EP1). Q<1 means that the second response was inhibited by the first one. For mechanical stimulation, whiskers were deflected by using a multiangle electromechanical stimulator. The stimulus waveform was ramp-and-hold trapezoids that produced 1.2 mm vibrissal displacements of 500 ms duration. The slope was 20 ms. The EPs in the punctum maximum of the MI contralateral to the stimulation (MI_C) and from its homotopic point in the other hemisphere (MI_I, usually 2 mm lateral and rostral from the bregma) were fed into a differential amplifier (Tektronix AM 502) and visualized on a Tektronix storage oscilloscope. Amplified responses were fed into a computer via an interface (Digidata 1200, pClamp 6.0.4. software, Axon Instruments) and stored for further processing. Averaged potentials were produced from registrations, each containing 60 trials.

Results

Animals

Although it was not the purpose of this experiment to make a detailed behavioural study on the effects of early treatment with MK-801, from the appearance of the adult animals it was obvious that the neonatal MK-801 treatment resulted in long-term effects. The body weight of the drug-treated animals on PND 90 was somewhat, but not significantly decreased: MK-801-treated group: 293.5±15.6 g, control group: 301.2±9.7 g (unpaired two-tailed *t*-test, P=0.1718; t=1.4). The behaviour of the MK-801-treated rats, however, was obviously different from that of the controls: they walked back and forth in the cage almost continuously with poor postural support.

Water maze performance

Experiment I

Even from the beginning, the performance during the eight training sessions revealed that the MK-801-treated animals needed somewhat more time to reach the platform. This tendency remained more or less unchanged during the eight sessions, though the difference in performance of the two groups was not significant in any one of the sessions (Fig. 1). The Repeated Measures ANOVA showed no significant difference between the groups (saline versus MK-801 treatment): $F(1,20)$= 0.9740; P=0.336, but the time as a within-subject factor was significant: $F(7,140)$=52.811, P<0.001. We did not find a group×time interaction: $F(7,140)$=0.611, P=0.746. It was interesting to observe that, in the first trial in the first session, the two groups needed approximately the same time to reach the platform. Later, the difference between the performances became larger, but did not attain the level of significance.

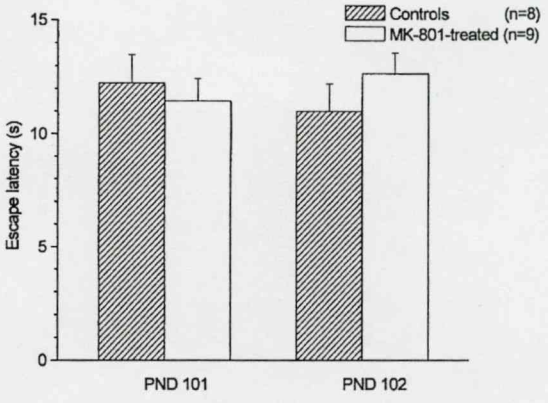

Fig. 2 Escape latencies for the two sessions of the visual cue task in experiment II. The MK-801-treated rats and the controls performed equally well in this task

The swimming strategies of the treated and control animals were not the same: the treated rats spent more time swimming round the pool, by the wall. The difference in performance, however, was not due to a difference in anxiety or swimming speed between the two groups. Taken together, therefore, the MK-801-treated rats were capable of learning in the course of the sessions, but their performance tended to be somewhat poorer than that of the controls.

Experiment II

To check the possibility of modification of the sensory and motor capabilities by MK-801 treatment, a visual cue task was given to the animals in both groups on PNDs 101 and 102. The visual task was performed equally well both by the control and the MK-801-treated animals (Fig. 2). Though the two-way ANOVA resulted in a significant interaction: $F(1,15)$=8.52 P=0.022, the minimal difference (1.2 s) between the two groups on PND 102 has no meaning from a biological point of view.

On the basis of the water maze analysis, it can be stated in general that the performances of the MK-801-treated animals in the spatial learning and memory task were slightly (but not significantly) poorer than that of the controls. However, the visual task was performed equally well both by the control and the treated rats.

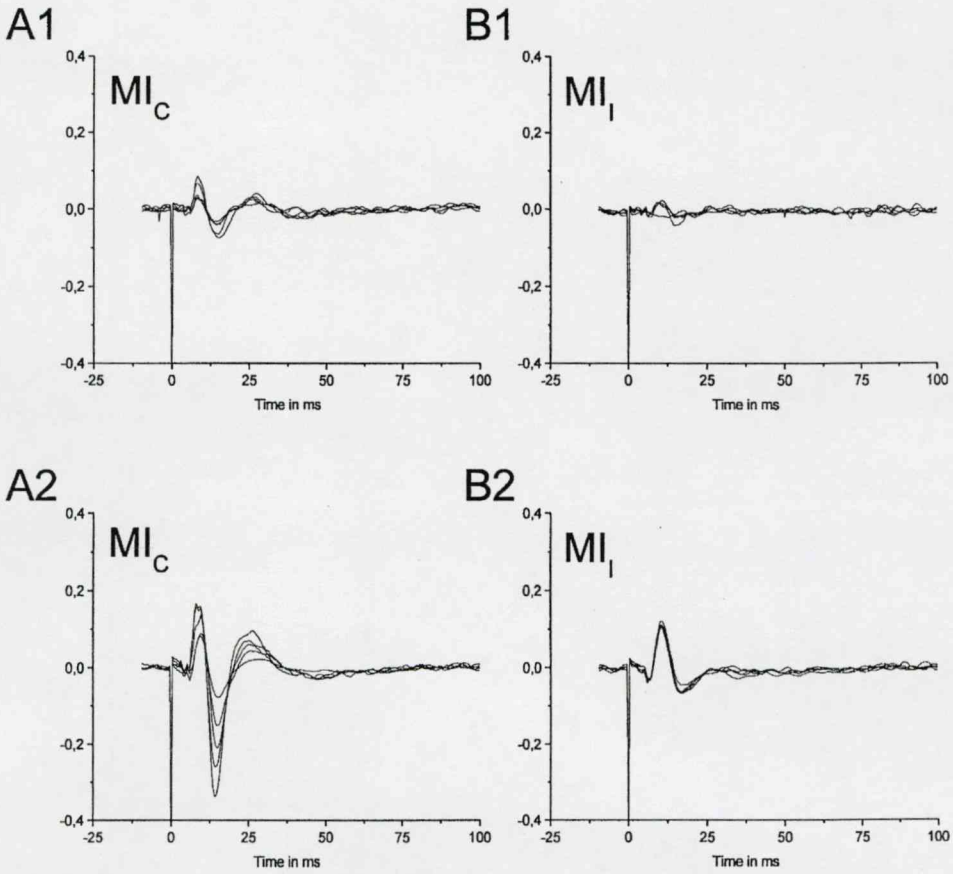

Fig. 3 Responses evoked in the MIs in both hemispheres of a control rat by right side electrical vibrissa pad stimulation. **A1** Evoked potentials (*EPs*) in the contralateral primary motor cortex (MI_C) recorded before, and **A2** 3 h after a facial nerve cut. **B1** EPs in the right side primary motor cortex ipsilateral to the stimulation (MI_I) before, and **B2** 3 h after vibrissa pad stimulation. *Ordinates* are in mV/div. Five (of 60) successive potentials were averaged in each set. (For more details, see Toldi et al. 1999)

Electrophysiology

The behavioural experiments were followed by electrophysiological recordings. In addition to the barrel field of the contralateral primary somatosensory cortex (SI_C), responses to trigeminal stimulation were also observed in the MI_C. In anaesthetized adult rats, both mechanical stimulation of the vibrissae and electrical stimulation of the whisker pad activate trigeminal afferents, which in turn produce complex response patterns in a subpopulation of neurons in the MI_C (Farkas et al. 1999). It has been shown that a facial nerve cut induces disinhibition in an extended area of the MI (Farkas et al. 2000), resulting in the facilitation of evoked responses (Toldi et al. 1999).

In the control rats, as described above, somatosensory EPs in the contralateral MI_C were rapidly modified by facial nerve transection. After 1 h, the amplitude of these potentials was significantly enhanced and the latencies of all the components had shortened. Responses with enhanced amplitudes could be observed throughout the 3- to 4-h recording session (Fig. 3A). The same was true for the MI_I (ipsilateral to the stimulation): in the control rats, stimulation of the trigeminal nerve or parts of it evoked potentials in the SI_C and MI_C, but very small if any potentials in the MI_I (Fig. 3B1). However, a few minutes after the facial nerve injury, EPs could also be elicited with enhanced amplitude in the MI_I. Their amplitude increased considerably within 1 h and remained high until the end of the experiments (3–4 h after denervation, Fig. 3B2). After the facial nerve transection, the EPs in the MIs were facilitated to different degrees in all of the control animals.

This was not the case in the rats treated with MK-801 as young animals. In all of these rats, trigeminal stimulation evoked potentials with high amplitude in the MI_C, and with small amplitude if any in the MI_I (Fig. 4A1, B1). This was similar to what was observed in the control rats. The facial nerve transection, however, did not facilitate the evoked responses in the MI in either hemisphere. In the majority of cases (60%), there was no change in amplitude or latency of the EPs following a facial nerve cut (Fig. 4A2, B2). In fact, in 40% of the cases studied, the amplitudes of the EPs decreased or vanished from both MIs. The Q-values were calculated in both the controls and the MK-801-treated animals. In all the controls, the studies with a paired-pulse paradigm revealed disinhibition (Q-values >1), which lasted in some cases for a short time (Fig. 5A), but in most cases for longer periods (see Table 1 and Farkas et al. 2000) following a facial nerve cut. However, there was hardly any increase in Q-values after the facial nerve cut in the MK-801-treated animals (Fig. 5B and Table 1). As the data in Table 1 show, in the controls, the N7x induces a consid-

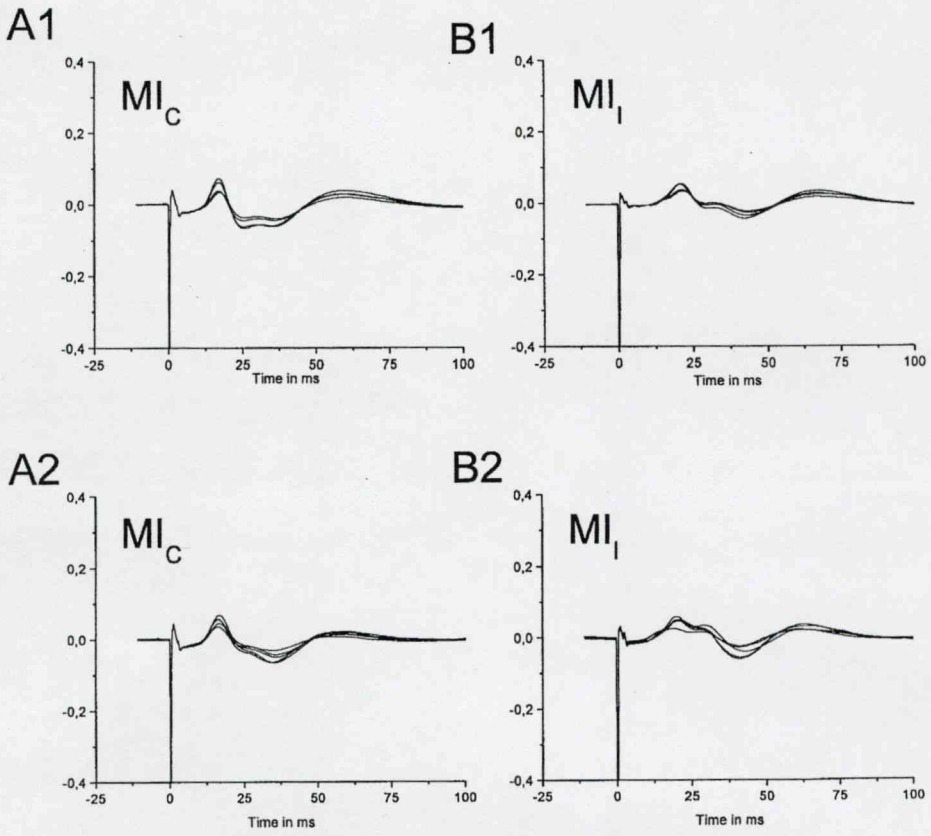

Fig. 4 Responses evoked in the MIs in both hemispheres in an MK-801-treated rat by electrical vibrissa pad stimulation on the right side. **A1** Evoked potentials (*EPs*) in the contralateral primary motor cortex (MI_C) before, and **A2** 3 h after a facial nerve cut. **B1** EPs in the primary motor cortex ipsilateral to the stimulation (MI_I) before, and **B2** 3 h after the facial nerve cut. The EPs were not changed after the facial nerve transection. *Ordinates* are in mV/div. Five (of 60) successive potentials were averaged in each set

Table 1 Changes in Q induced by facial nerve denervation (N7x). Q-values (mean) were evaluated in 3×5 min blocks: just before N7x (basic level), 5–10 and 40–45 min after N7x, respectively. *n* (=5): number of 60 paired responses

Groups	Before N7x (basic level) (*n*)	5–10 min after N7x (*n*)	40–45 min after N7x (*n*)	Q change (in%) relative to the basic level		*P*-value	
				10 min	45 min	Bonferroni adjustment for multiple comparisons	
						10 min	45 min
Controls							
1	0.45	0.94	0.83	+108	+84	<0.001	<0.001
2	0.34	0.70	1.06	+105	+211		
3	0.39	0.64	0.86	+64	+105		
4	0.60	1.32	1.03	+120	+71		
5	0.44	1.04	1.04	+136	+45		
6	0.35	0.64	0.79	+82	+125		
7	0.52	1.13	0.93	+117	+78		
8	0.56	1.00	1.08	+78	+92		
MK-801 treated rats							
1	0.71	0.69	0.38	–2	–46	0.194	0.276
2	0.43	0.73	0.55	+69	+27		
3	0.44	0.39	0.50	–11	+13		
4	0.49	0.83	0.72	+69	+46		
5	0.40	0.44	0.68	+10	+70		
6	0.37	0.37	0.79	–	+113		
7	0.43	0.59	0.42	+37	–2		

erable disinhibition (elevation in Q-values) shortly after (5–10 min) denervation, this disinhibition lasting for a long time (40–45 min). This is not the case in the MK-801-treated animals: after N7x, moderately increased Q-values were observed in most animals (with Q<1 in all cases), while even decreases in Q-values could be detected in some animals. The Repeated Measures ANOVA revealed a significant group×time interaction: $F(2,26)=8.819$, $P=0.001$. This is an indication that the Q-values in the controls are changed signifi-

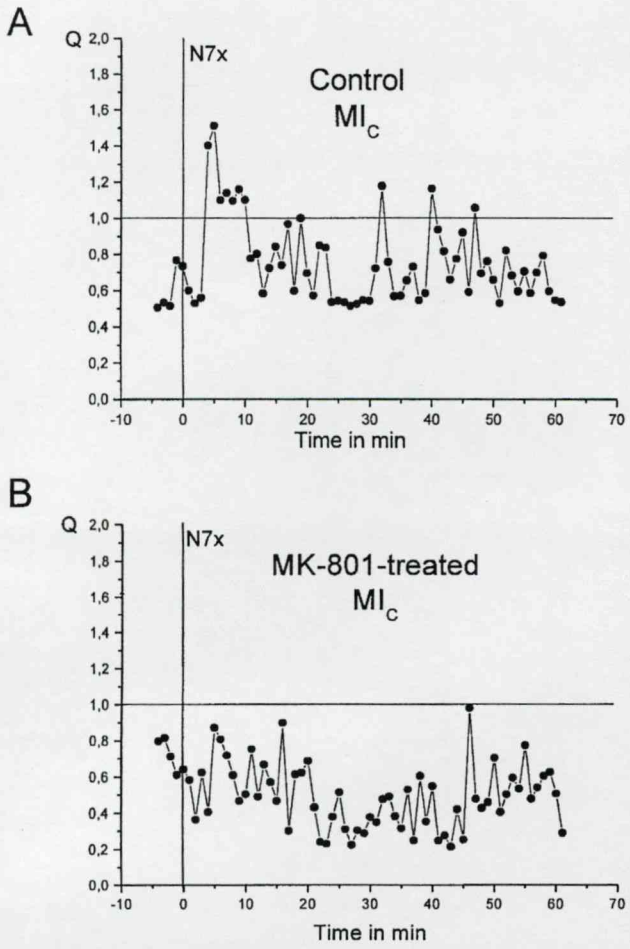

Fig. 5A, B Q-values calculated from the paired-pulse paradigm in the contralateral MI of a control and of an MK-801-treated animal, displayed as a function of time. **A** In the control animal, facial nerve transection produced a short (~4 min) and, with some delay, a longer-lasting (~35–40 min) elevation of Q. **B** In the MK-801-treated animal, transection of the facial nerve did not cause cortical disinhibition, e.g. the Q-values remained <1

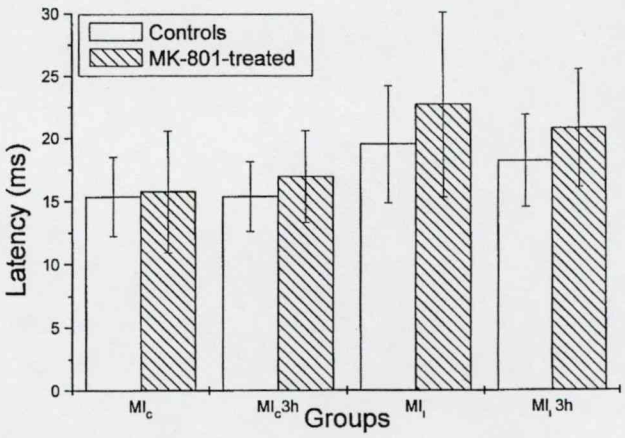

Fig. 6 Mean latencies of the evoked potentials (*EPs*) (first positive peak) in the different animal groups. The mean latencies of the treated animals were somewhat longer than those for the controls, though these differences were not significant (independent *t*-test, $P>0.05$). *Bars* represent means±SD. MI_C and MI_I mean latencies of EPs in the primary motor cortex contralateral and ipsilateral, respectively, to the stimulation and nerve injury. $MI_C3\ h$ and $MI_I3\ h$ mean the latencies of the evoked responses 3 h after facial nerve transection

cantly after N7x, but not those in the MK-801-treated animals.

Minimal differences in the latencies of the EPs were observed in the controls and in the treated animals. The treated animals had EPs with somewhat longer latencies (Fig. 6). In the control animals, the mean latencies of the EPs recorded from the MI_C before and 3 h after the facial nerve cut were 15.36±3.142 ms and 15.382±2.774 ms, while in the MI_I they were 19.533±4.669 ms and 18.210± 3.664 ms. In the treated animals, the mean latencies of the EPs recorded from the MI_C before and 3 h after the facial nerve cut were 15.770±4.845 ms and 16.949± 3.658 ms, while in the MI_I they were 22.708±7.384 ms and 20.816±4.714 ms. For further analysis of the amplitudes and latencies of EPs recorded in the contralateral motor cortices of five controls and five MK-801-treated animals before and 3 h after N7x, a repeated measures ANOVA was carried out. A significant interaction was found for the amplitudes: $F(1,8)=5.701$, $P=0.044$, but not for the latencies.

Discussion

The effects of chronic neonatal MK-801 treatment on the spatial and non-spatial learning of adult rats have been extensively studied (McLamb et al. 1990; Gorter and de Bruin 1992; Mickley et al. 1992; Tandon et al. 1996; Griesbach and Amsel 1998). Some authors have reported that a chronic NMDA receptor blockade during the neonatal period leads to long-lasting disturbances of the hippocampal functions, i.e. to the impairment of various learning and memory tasks (Gorter and de Bruin 1992); in contrast, others did not find long-term effects on behaviour (e.g. Tandon et al. 1996). Apart from differences in the amount of MK-801 applied, there were differences in the application methods, testing paradigms and results, and mainly in their interpretation. Despite these differences, most of the authors agreed that, because of its crucial role in development, the perinatal blockade of NMDA receptors might have behavioural consequences when tests are made at a more advanced age.

This view is particularly supported by those observations which reveal that NMDA antagonists may increase neurodestruction in mature brain undergoing slowly progressing neurodegeneration (Takadera et al. 1999; Ikonomidou et al. 2000; Pohl et al. 1999). The neurotoxic effect of MK-801 is even more serious in the perinatal age: the blockade of NMDA receptors for only a few hours during late fetal or early neonatal life triggers widespread apoptotic neurodegeneration in the developing rat brain (Ikonomidou et al. 1999).

We did not set out to perform another detailed behavioural study. Rather, we wanted to find a way to cause a minimal impairment in behaviour, which was based on learning and memory functions without interfering with physical capabilities, and to test whether this influences experimentally induced cortical plasticity that is detectable by electrophysiological methods.

First of all, we had to find a dose of MK-801 that resulted in a slight impairment of the performance in the water maze task. We started the treatment with relatively high doses of MK-801 (0.5 or 1 mg/kg), but this led to impaired food consumption, a high loss in body weight, akinesia, and a high level of mortality among the young animals (only 67% and 51% of the treated animals survived PND 15, respectively). These results are not detailed here. Finally, we turned to the treatment of newborn rats with a dose of 0.1 mg/kg MK-801, which resulted in a very slight impairment of the performance in the water maze task and produced hyperactivity, but did not impair the performance of the visual cue response of the adult animals.

In experiment I, the performance in the water maze was quite similar to that observed by Gorter and de Bruin (1992), though those authors used higher doses of MK-801, which resulted in greater differences between the performances of the treated and control groups, whereas we aimed for the slightest impairment in performance which could still be detected.

As a result of the neonatal treatment with a low dose of MK-801, the spatial learning of the adults was slightly reduced, but the difference was not significant.

The visual task (experiment II) was performed equally well by the controls and the treated rats. This suggests that the sensory and motor capabilities were not affected by the treatment. A deficit was found only in the spatial task performance of the adults. Similar conclusions were drawn by Gorter and de Bruin (1992).

Recent studies support the hypothesis that MK-801 mainly influences learning and memory in a NMDA receptor-dependent manner (Bordi et al. 1996; Ahlander et al. 1999; Norris and Foster 1999).

It has been suggested that MK-801 applied during a period in which the NMDA receptors are involved in developmental changes has effects such as a learning impairment which may be related with structural alterations in neuronal development (Griesbach and Amsel 1998). If this holds true, it is unlikely that such effects are limited to the hippocampus. NMDA receptors play an important role in synaptic plasticity in various cortical areas, e.g. the motor cortex (Aroniadou and Keller 1993).

It has been shown that a component of the field potentials evoked in the MI of rat, and its potentiation, are mediated by NMDA receptors (Hess and Donoghue 1994; Hess et al. 1994). For this reason, our electrophysiological studies were performed in the motor cortex rather than the hippocampus.

Simple recordings of EPs in the MI cortices did not reveal significant differences between the controls and the MK-801-treated animals. Therefore, we tested a more complex phenomenon. The plasticity of evoked responses induced by facial nerve injury can be tested by the paired pulse paradigm. Although there is no evidence that NMDA receptors are involved in the recently described potentiation of somatosensory evoked responses in the MI after unilateral transection of the facial nerve (Toldi et al. 1999; Farkas et al. 2000), it was interesting to test whether perinatal treatment with MK-801 interferes with spatial learning and the potentiation of cortical responses in adult rats. In the control animals, the responses evoked in the MIs of both hemispheres by continuous 1 Hz trigeminal stimulation were facilitated after facial nerve transection. This was not the case with the MK-801-treated animals. In a majority of the cases studied, the evoked responses did not change, while in 40% of the cases, continuous stimulation reduced the evoked responses recordable after facial nerve transection.

Under these conditions, an in vitro study proved the occurrence of long-term potentiation in intrinsic horizontal pathways in the MI (Hess and Donoghue 1994). Our experimental paradigm was different. The potentiation of evoked responses was observed in vivo in anaesthetized animals; we used 1 Hz continuous peripheral stimulation instead of theta-burst stimulation. In both cases, however, the potentiation indicated a transient reduction of inhibition. This was achieved by Hess and Donoghue (1994) by application of the GABA-A receptor antagonist bicuculline, while in our case (Farkas et al. 2000) facial nerve transection decreased the inhibition, as reported by Garraghty et al. (1991).

This suggests that inhibition may act as a gate to permit modification in the efficacy of horizontal excitatory connections. However, both the literature and our own results suggest that the reduced inhibition is not a sufficient condition for the development of MI plasticity. Although there is no direct evidence that potentiation of the evoked responses in the MI requires the participation of NMDA receptors, it has been suggested (Qiu et al. 1990; Hess et al. 1994) that these receptors can probably be modified by neonatal MK-801 treatment.

Whatever the mechanism, we have presented an example that a slight impairment in learning and memory function may be accompanied by a hidden defect in cortical function, which can be disclosed with appropriate electrophysiological methods, e.g. paired pulse stimulation.

Acknowledgements The present research was supported in part by Hungarian grants (FKFP 1195/1997, NKFP 1/027 and OTKA T031893) and a NATO grant (LST. LCG. 976235). T.F. was a Humboldt Fellow (IV-UNG 1068032 STP), and later Békésy György Postdoctoral Fellow (BÖ 211/2001).

References

Ahlander M, Misane I, Schott PA, Ogren SO (1999) A behavioral analysis of the spatial learning deficit induced by the NMDA receptor antagonist MK-801 (dizocilpine) in the rat. Neuropsychopharmacology 21:414–426

Aroniadou VA, Keller A (1993) The patterns and synaptic properties of horizontal intracortical connections in the rat motor cortex. J Neurophysiol 70:1553–1569

Bordi F, Marcon C, Chiamulera C, Reggiani A (1996) Effects of the metabotropic glutamate receptor antagonist MCPG on spatial and context-specific learning. Neuropharmacology 35:1557–1565

Farkas T, Kis Z, Toldi J, Wolff JR (1999) Activation of the primary motor cortex by somatosensory stimulation in adult rats is mediated mainly by associational connections from the somatosensory cortex. Neuroscience 90:353–361

Farkas T, Perge J, Kis Z, Wolff JR, Toldi J (2000) Facial nerve injury-induced disinhibition in the primary motor cortices of both hemispheres. Eur J Neurosci 12:2190–2194

Garraghty P, LaChica E, Kaas J (1991) Injury-induced reorganization of somatosensory cortex is accompanied by reductions in GABA staining. Somatosens Motor Res 8:347–354

Gorter JA, de Bruin JPC (1992) Chronic neonatal MK-801 treatment results in an impairment of spatial learning in the adult rat. Brain Res 580:12–17

Griesbach GS, Amsel A (1998) Immediate and long-term effects of neonatal MK-801 treatment on nonspatial learning. Proc Natl Acad Sci USA 95:11435–11439

Hess G, Donoghue JP (1994) Long-term potentiation of horizontal connections provides a mechanism to reorganize cortical motor maps. J Neurophysiol 71:2543–2547

Hess G, Jacobs KM, Donoghue JP (1994) *N*-Methyl-D-aspartate receptor mediated component of field potentials evoked in horizontal pathways of rat motor cortex. Neuroscience 61:225–235

Ikonomidou C, Bosch F, Miksa M, Bittigau P, Vockler J, Dikranian K, Tenkova TI, Stefovska V, Turski L, Olney JW (1999) Blockade of NMDA receptors and apoptotic neurodegeneration in the developing brain. Science 283:70–74

Ikonomidou C, Stefovska V, Turski L (2000) Neuronal death enhanced by *N*-methyl-D-aspartate antagonists. Proc Natl Acad Sci USA 97:1285–12890

McLamb RT, Williams LR, Nanry KP, Wilson WA, Tilson HA (1990) MK-801 impedes the acquisition of a spatial memory task in rats. Pharmacol Biochem Behav 37:41–45

Mickley GA, Ferguson JL, Nemeth TJ (1992) Serial injections of MK-801 (dizocilpine) in neonatal rats reduce behavioral deficits associated with X-ray-induced hippocampal granulare cell hypoplasia. Pharmacol Biochem Behav 43:785–793

Norris CM, Foster TC (1999) MK-801 improves retention in aged rats: implications for altered neural plasticity in age-related memory deficits. Neurobiol Learn Mem 71:194–206

Pohl D, Bittigau P, Ishimaru MJ, Stadthaus D, Hübner C, Olney JW, Turski L, Ikonomidou C (1999) *N*-Methyl-D-aspartate antagonists and apoptotic cell death triggered by head trauma in developing rat brain. Proc Natl Acad Sci USA 96:2508–2513

Qiu X, O'Donoghue DL, Humphrey DR (1990) NMDA anatagonist (MK-801) blocks plasticity of motor cortex maps induced by passive limb movement. Soc Neurosci Abstr 16:422

Sanes JN, Donoghue JP (2000) Plasticity and primary motor cortex. Annu Rev Neurosci 23:393–415

Takadera T, Matsuda I, Ohyashiki T (1999) Apoptotic cell death and caspase-3 activation induced by *N*-methyl-D-aspartate receptor antagonists and their prevention by insulin-like growth factor I. J Neurochem 73:548–556

Tandon P, Liu Z, Stafstrom CE, Sarkisian M, Werner SJ, Mikati M, Yang Y, Holmes GL (1996) Long-term effects of excitatory amino acid antagonists NBQX and MK-801 on the developing brain. Brain Res Dev Brain Res 95:256–262

Toldi J, Farkas T, Perge J, Wolff JR (1999) Facial nerve injury produces a latent somatosensory input through recruitment of the motor cortex in the rat. NeuroReport 10:2143–2147

The modulatory effect of estrogen on the neuronal activity in the barrel cortex of the rat. An electrophysiological study

Zsolt Kis, Dénes Budai,[1] Gábor Imre, Tamás Farkas, Szatmár Horváth and József Toldi[CA]

Department of Comparative Physiology, University of Szeged, H-6701 Szeged, POB 533; [1]Department of Biology, Juhász Gyula College, University of Szeged, Szeged, Hungary

[CA]Corresponding Author

Received 19 April 2001; accepted 1 June 2001

In acute experiments, the effects of iontophoretically applied 17β-estradiol hemisuccinate on the activity of the primary somatosensory cortical neurons were studied in ovariectomized rats by extracellular single-unit recording. 17β-Estradiol increased both the spontaneous and the vibrissa deflection-evoked responses, with an average latency of 24 min. It is suggested that this relatively long latency of the 17β-estradiol effect is based not so much on membrane mechanisms as on genomic mechanisms. *NeuroReport* 12:2509–2512 © 2001 Lippincott Williams & Wilkins.

Key words: Barrel cortex; Estradiol; Iontophoresis; Neuronal plasticity; Somatosensory system; Steroids

INTRODUCTION

Although the classic function of estrogen is to act at the level of the hypothalamo-pituitary-gonadal axis and uterus to promote a full reproductive function, for many years it has been known that steroids also play an important role in plastic changes in the CNS. Most of these observations were made on the hypothalamus [1–3]. There have also been reports on the neuroplastic effects of estradiol in the hippocampus and in other structures of the CNS [4,5]. Simerly *et al.* [6] found estrogen receptor (ER) mRNA-containing cells in the different structures of the rat brain, including the somatosensory (barrel) cortex, and especially in layer IV.

Using *in situ* hybridization histochemistry, Shughrue *et al.* [7] recently demonstrated that the cerebral cortex contains both kinds of ER mRNAs, but that hybridization signal for ER α mRNA is very weak compared with that for ER β mRNA. They found ER β mRNA-containing perikarya in laminae IV–VI of the cortex [7].

Despite the strict topographic organization of the posteromedial barrel subfield (PMBSF) in the primary somatosensory cortex [8,9] it has a significant capacity to undergo functional changes, even in adulthood [10–12]. If the ERs are present, and it is presumed that they have a functional role, possibly involving neuronal plasticity, the pertinent question to be asked at this stage is whether estrogen can alter the neuronal physiology in the local circuit of the extrahypothalamic CNS. The neurons in the PMBSF which respond with short latency to contralateral vibrissa stimulation, were chosen as test site because they are well characterized both anatomically and electrophysiologically [13,14], and contain ERs [7]. This is a good model system with which to test the effects of 17β-estradiol on both spontaneous and evoked cortical neuronal activity. In particular, the conceptual idea tested here was whether estrogen can modulate the responsiveness of the barrel cortex neurons to peripheral stimulation and, in the event of a positive answer, whether this effect involves genomic or membrane mechanisms.

MATERIALS AND METHODS

Surgical procedures: The experimental procedures used in this study followed the protocol for animal care approved by both the Hungarian Health Committee (1998) and the European Communities Council Directives (86/609/EEC). Three-month-old ovariectomized Sprague–Dawley rats (23 animals, 2–5 weeks after ovariectomy) were anesthetized with a mixture of Ketavet (10 mg/100 g) and Rompun (xylazine, 0.8 mg/100 g). The animals were secured in a stereotaxic headholder (David Kopf) that provided access to the primary somatosensory cortex. Craniotomy was performed on the left hemisphere over the PMBSF. The dura mater was removed and the core temperature was maintained at 37.0–37.5°C with an automatic heating system. After surgery, the animals were kept at rest for 1 h.

Electrophysiology: Right side individual whiskers were deflected by using a multiangle electromechanical stimulator [15]. Before vibrissal stimulation, all of the vibrissae on the right side were cut to a length of 15 mm. The arm of the stimulator was attached to a vibrissa 10 mm from the base of the hair. The stimulus wave forms were ramp-and-

hold trapezoids that produced 1.2 mm vibrissal displacements of 480 ms duration. The slope was 20 ms. Compound recording/iontophoresis microelectrodes were constructed from a seven-barreled array of thin-wall borosilicate glass capillary tubing (1.5 mm o.d., 1.12 mm i.d.; WPI, Sarasota, FL). The center barrel contained a 7 µm carbon fiber, creating a low impedance (0.4–0.8 MΩ at 1 kHz) recording electrode. Drugs were ejected iontophoretically from the surrounding six barrels of the combined microelectrode containing one of the following freshly made solutions: 100 mM sodium L-glutamate (GLUT, Sigma) in 100 mM NaCl (pH 8.0), 100 mM GABA (Sigma) in 100 mM NaCl (pH 4.0), and 100 mM 17β-estradiol hemisuccinate (E2, Sigma) in 100 mM NaCl (pH 7.2). GLUT was ejected at −50 nA, 30 s, E2 at −100 nA, 60 s, and GABA at +50 nA, 30 s. Retaining currents in the opposite direction were used in the interval 3–10 nA. Microiontophoresis was performed with a three-channel constant current generator developed in-house.

The electrodes were advanced in 3–5 µm steps, by means of a Narishige (MO-8) hydraulic micromanipulator. Extracellular action potentials from the barrel cortex neurons were amplified and filtered (30 Hz to 8 kHz) with an ExAmp-20KB amplifier (Kation Scientific, Minneapolis, MN). Neuronal activity was displayed on a Tektronix storage oscilloscope (5103N). At the correct recording site and depth, each vibrissa bend evoked vigorous on–off activities with 1 or 2 spikes as on and off responses, respectively. Amplified unit responses were fed into a computer via an interface (Digidata 1200, pClamp 6.0.4. software, Axon Instruments) and stored for further processing. Peristimulus time histograms (PSTHs, bin width: 2 ms) were produced from registrations each containing 50 trials. The rate of neuronal activity (in number of spikes per second, mean values and s.d.) was evaluated twice in each minute, both before and after 17β-estradiol application. The unpaired two-tailed *t*-test was used to set the probability level at >95% for the difference between the activities of 20 s samples taken twice in each minute.

RESULTS

Unit responses evoked at a depth of 800–1200 µm in the barrel cortex by vibrissal deflections were similar to those already described: the cells within a barrel responded best to one vibrissa, the principal vibrissa (Fig. 1), but could commonly be driven less effectively and with a longer latency by some surrounding vibrissae [12,14]. First of all, the effectiveness of the iontophoresis was controlled by GABA and GLUT application to those neurons which seemed to be recordable reliably and for long enough. In the course of the experiments, we tested the activity of >70 neurons, but analyzed only those data when the unit activity could be followed for ≥45–50 min. The *in situ* study of the electrophysiological activity of barrel cortex neurons combined with drug application by iontophoresis can be a difficult task, especially when a substance (such as estradiol) is applied which influences the neuronal activity with a long delay. We had to hold the cells for ≥45–50 min. This is the reason why we fully analyzed only 14 neurons, though we started the analysis of >70 neurons.

Effects of GABA and GLUT: Iontophoretic application of GABA (+50 nA, 30 s) resulted in immediate decreases in both spontaneous discharges (to 6–10%) and evoked unit activity (Fig. 2a,b). In contrast, the application of GLUT (−50 nA, 30 s) increased both the spontaneous and the evoked neuronal discharges (Fig. 2c,d). The spontaneous activity increased by 350–400% within 30 s after GLUT application.

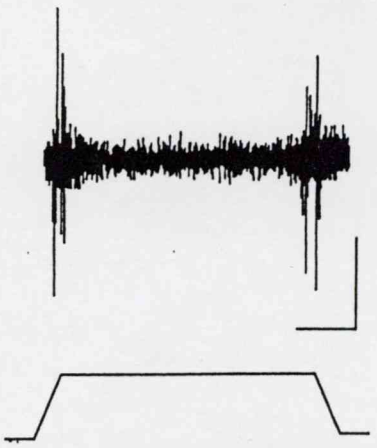

Fig. 1. On–off responses of a neuron in the barrel cortex, evoked by contralateral vibrissa deflection. Extracellular-unit recordings were made with a seven-barreled carbon fiber microelectrode. The trapezoid shows the deflection of the vibrissa from the resting position in a caudal direction. Calibration: 100 µV, 100 ms.

Effect of estradiol on the activity of barrel cortex neurons: In all those cases when unit activities could be followed for a sufficient time, the spontaneous activity of the neurons increased after 17β-estradiol iontophoresis (−100 nA, 60 s) in five of 14 neurons. By 25–35 min after iontophoresis, in four of five responding cells, the estradiol-evoked excitation was increased by 208–360% over the control level. (One responding cell had an extremely long latency: 38 min, see later). Similarly, both on and off components of the responses evoked by vibrissa deflection were facilitated (Fig. 3a,b). As an example, the data observed on one of the five neurons 10 min before and 30 min after estradiol application are given in Table 1. The spontaneous activity increased by 214%, and the evoked on and off responses by 262% and 274%, respectively. All changes were highly significant. Similar results were observed for each of five neurons which responded to 17β-estradiol. It was important to determine the delay of the response to estradiol. As detailed above, the firing rates (calculated as number of spikes/s) were determined twice in each min. The first non-transient significant change in firing rate was regarded as the onset of the response to 17β-estradiol. The delays of the five responses were as follows: 17 min, 18 min, 38 min, 24 min and 23 min. On average, the delay of the responses to 17β-estradiol was 24 min. As opposed to the effect of GABA or GLUT, the 17β-estradiol-induced increase in neuronal activity was prolonged, and lasted until we lost the cell. Unfortunately, this means that we cannot judge how long the responses lasted. We can establish only that the responses were elevated for the time of recording (for ≥15–25 min after the onset). The rates of responses were not uniformly high; they peaked and then attenuated but

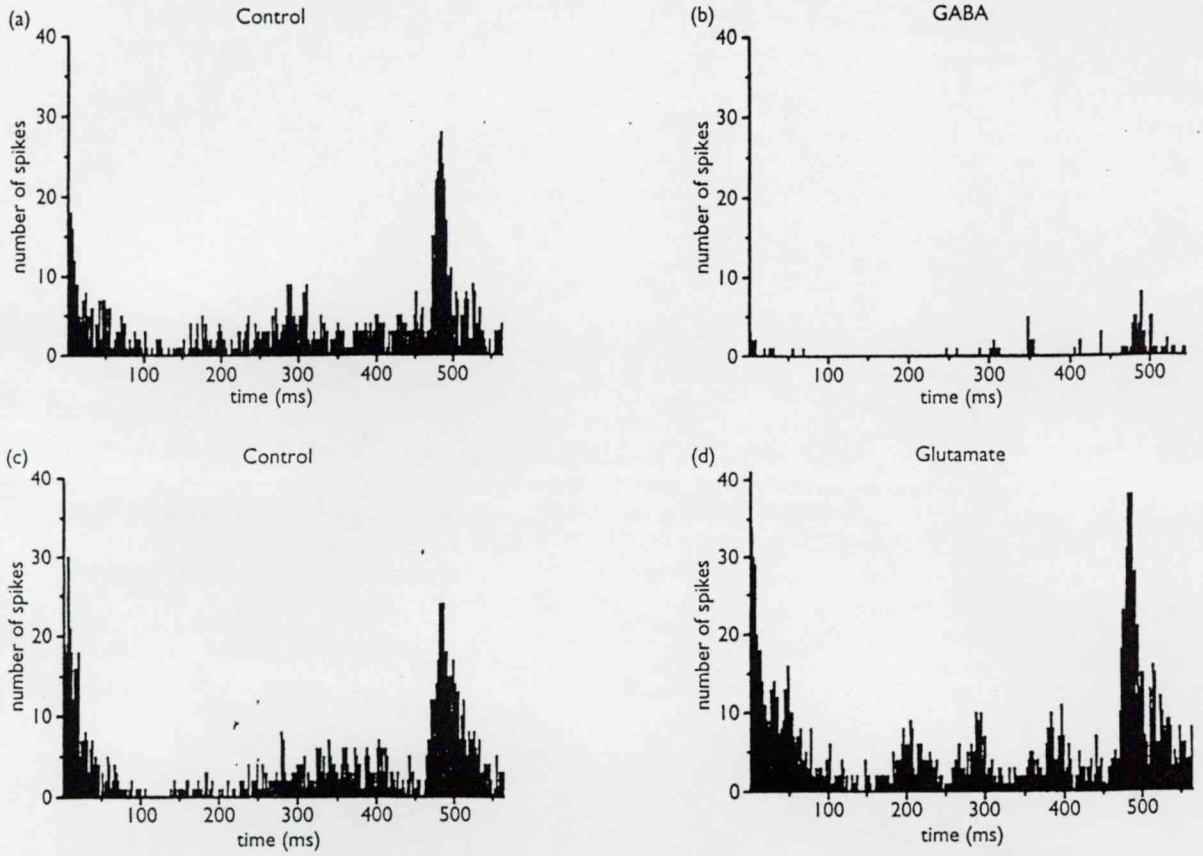

Fig. 2. Peristimulus time histograms (PSTHs) of evoked activities observed in the barrel cortex. On–off neuronal responses were evoked by contralateral vibrissal deflection (**a**) before and (**b**) 30 s after iontophoretic application of GABA. (**c**) On–off responses before and (**d**) 30 s after Na-glutamate iontophoresis.

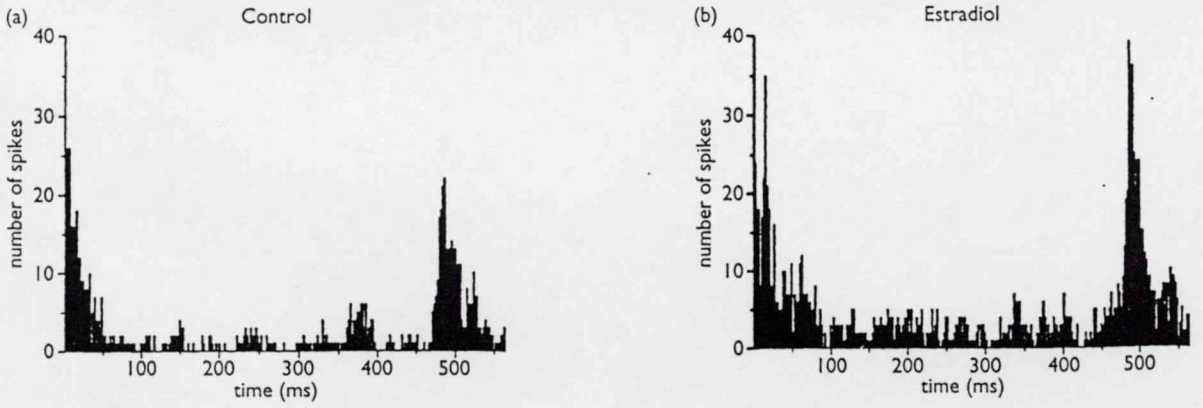

Fig. 3. Peristimulus time histograms (PSTHs) of a neuron in the barrel cortex, observed before (**a**), and 38 min after iontophoretic application of 17β-estradiol hemisuccinate (**b**).

remained above the control level during the time of registration. The remainder of the fully tested neurons (9) did not respond to E2.

DISCUSSION

The presented results clearly show that, under controlled circumstances (previous GABA and GLUT application), 17β-estradiol is able to increase significantly both the spontaneous and the evoked activity of some of the neurons in the barrel cortex within 25–35 min.

In the present decade, several groups have demonstrated effects of estrogen on the neuronal plasticity in both hypothalamic and extrahypothalamic structures [1–5]. It has also been shown that estrogen plays a key role in many other processes of the CNS, including neuroprotection [16,17].

Table 1. Changes in spontaneous and evoked neuronal activities (numbers of spikes per second) of a barrel cortex neuron before and after estrogen application.

	Spontaneous activity	Evoked reponses	
		On	Off
Control	29.8 ± 9.0*	111.2 ± 15.8**	153.8 ± 17.6***
30 min after estradiol	63.8 ± 2.4*	291 ± 14.0**	420 ± 11.5***

Neuronal activities (mean ± s.d.) were calculated from the 20 blocks of 560 ms activity samples taken 10 min before and 30 min after 17β-estradiol iontophoresis. * $p = 0.0032$; ** $p = 0.0001$, *** $p < 0.0001$.

Great efforts have recently been made to elucidate the mechanisms of the multiple actions of steroid hormones, with particular focus on a differentiation between its genomic and non-genomic effects [18,19].

The latency of the neuronal excitation induced by estrogen was found in this study to be 25–35 min. In cerebellar Purkinje cells, the potentiation of responses was earlier observed as soon as 5–10 min post-estradiol [20,21]. It is suggested that the 20–25 min latency of the effect of 17β-estradiol is based not so much on membrane mechanisms as on genomic mechanisms [22]. However, it is probably an over-simplification to categorize the effects of estrogen into genomic and non-genomic mechanisms merely on the basis of the latency. First, some genomic effects of steroids can be very rapid: within 10–20 min [23]. Second, the ability of the liganded intracellular E2 receptor to stimulate membrane processes suggests cross-talk between the genomic and membrane receptor pathways [19,24]. In spite of these possibilities, the long latency observed for the estrogen effect in this study suggests that it is based on genomic mechanisms.

Another important question is the function of estrogen in the barrel cortex. If it is presumed that estrogen has any role in the somatosensory cortex, the presence of estrogen receptors must be proved. This was done recently [7]. The next step was to demonstrate the functioning of estrogen in that cortical area. This has been done in the present study. We found only five out of the fully analyzed 14 cells (36%) that responded to estrogen. This fits well with the relatively low density of ERs in the cortex [7]. Apart from the latency, the facilitatory effect of estrogen on cortical neurons demonstrated here is comparable to findings in the hippocampus [25] and Purkinje cells [20,21]. Unfortunately, at the moment we do not know the site of action of estrogen within the cortex. It could well be that estrogen does not act directly on the recorded barrel cortical neuron responding with short latency to the principal vibrissa stimulation, but on a GABAergic interneuron, for instance. This mechanism is known in the hypothalamic arcuate nucleus, where inhibitory interneurons having ERs respond to estrogen by withdrawing their presynaptic axon terminals, resulting in decreased GABAergic axosomatic synapses [26], and consequently, in the increased firing of principal arcuate neurons [27]. There is another possibility: neuroactive steroids are potent positive allosteric modulators of GABAA receptors because they increase the frequency or duration of openings, or both, of the GABA-gated Cl^- channels [19]. If this takes place on a GABAergic interneuron, it could result in disinhibition of the recorded cortical neuron. This is not probable, however, because of the relatively long delay of estrogen-induced facilitation.

Whatever the mechanism, as far as we know, the observation presented here is the first demonstration of an estrogen-induced change in excitability of the neurons in the rat cortex. Our ongoing studies are designed to elucidate the possible function of estrogen in the recovery processes following cortical lesion induced by focal ischemia.

CONCLUSION

This study is the first to demonstrate the effect of 17β-estradiol on neuronal single-unit activity evoked by peripheral stimulation in the barrel cortical area of the primary somatosensory cortex. About one-third of the tested cortical neurons displayed changes (all facilitated) in both spontaneous and evoked activity. The late onset of the action of estradiol makes it unlikely that the changes are consequences of direct membrane effects.

REFERENCES

1. Frankfurt M. *Ann NY Acad Sci* **743**, 45–60 (1994).
2. Párducz A, Pérez J and Garcia-Segura LM. *Neuroscience* **53**, 395–401 (1993).
3. Naftolin F, Mor G, Horváth TL *et al. Endocrinology* **137**, 5576–5580 (1996).
4. VanderHorst VG and Holstege G. *J Neurosci* **17**, 1122–1136 (1997).
5. Wooley CS. *Hormone Behav* **34**, 140–148 (1998).
6. Simerly RB, Chang C, Muramatsu M and Swanson LW. *J Comp Neurol* **294**, 76–95 (1990).
7. Shughrue PJ, Lane MV and Merchenthaler I. *J Comp Neurol* **388**, 507–525 (1997).
8. Welker C. *Brain Res* **26**, 259–276 (1971).
9. Simons DJ. *J Neurophysiol* **41**, 798–820 (1978).
10. Kossut M. *Prog Neurobiol* **39**, 389–422 (1992).
11. Kóródi K and Toldi J. *Neuroreport* **9**, 771–774 (1998).
12. Kis ZS, Farkas T, Rábl K. *et al. Exp Brain Res* **126**, *259–269 (1999).*
13. Welker C and Woolsey TA. *J Comp Neurol* **158**, 437–453 (1974).
14. Armstrong-James MA, Fox K and Das Gupta A. *J Neurophysiol* 68, 1345–1358 (1992).
15. Toldi J, Fehér O, Antal A. *et al. Neuroscience* **37**, *675–683 (1990).*
16. Garcia-Segura LM, Azcoitia I and Doncarlos LL. *Prog Neurobiol* 63, 29–60 (2001).
17. Liao S, Chen W, Kuo J. *et al. Neorosci Lett* **297**, *159–162 (2001).*
18. Falkenstein' E, Tillmann HC, Christ M. *et al. Pharmacol Rev* **52**, *513–556 (2000).*
19. Zakon HH. *Trends Neurosci* **21**, 202–207 (1998).
20. Smith SS. *Brain Res* **503**, 354–357 (1989).
21. Smith SS, Waterhouse BD and Woodward DJ. *Brain Res* **422**, 40–51 (1987).
22. McEwen BS. *Trends Pharmacol Sci* **12**, 141–147 (1991).
23. Mosher K, Young D and Munck A. *J Biol Chem* **246**, 246–259 (1971).
24. Rupprecht R and Holsboer F. *Trends Neurosci* **22**, 410–416 (1999).
25. Wong M and Moss RL. *Brain Res* **543**, 148–152 (1991).
26. Garcia-Segura LM, Chowen JA, Párducz A *et al. Prog Neurobiol* **44**, 279–307 (1994).
27. Kis ZS, Horváth SZ, Hoyk ZS *et al. Neuroreport* **10**, 3649–3652 (1999).

Acknowledgements: This work was supported by grants from OTKA (T031893) and NKFP (1/027)

NeuroReport 10, 3649–3652 (1999)

Estrogen effects on arcuate neurons in rat. An *in situ* electrophysiological study

Zsolt Kis,[CA] Szatmár Horváth, Zsófia Hoyk,[1] József Toldi and Árpád Párducz[1]

Department of Comparative Physiology, József Attila University, POB 533, H-6701 Szeged; [1]Institute of Biophysics, Biological Research Center, Szeged, Hungary

[CA]Corresponding Author

IN acute experiments, the effects of i.p. 17β-estradiol on the activity of arcuate neurons were studied in ovariectomized rats. 17β-Estradiol (100 μg/100 g, i.p.) increased the spontaneous activity of the observed arcuate neurons with a latency of 20–25 min. In some neurons spontaneous activity could be influenced by stimulation of the olfactory and somatosensory systems. Activation of the trigeminal system significantly increased the spontaneous activity of the studied units, while stimulation of the accessory olfactory bulb decreased it, both with and without 17β-estradiol treatment. It is suggested that the 20–25 min latency of the 17β-estradiol effect is based not so much on membrane as on genomic mechanisms. This suggestion is supported by immunocytochemical studies: 17β-estradiol treatment significantly decreased the number of GABA-positive axo-somatic synapses in the arcuate nucleus. *NeuroReport* 10:3649–3652 © 1999 Lippincott Williams & Wilkins.

Key words: Arcuate nucleus; 17β-Estradiol; GABA; Neuronal activity; Neuronal plasticity; Steroids

Introduction

The neuroendocrine regulation of gonadotropin secretion in female animals is known to be under the control of the predominant inhibitory neurotransmitter in the brain, GABA [1]. The activity of the GABA system (which represents about 50% of the hypothalamic neuronal population) has been reported to be the key regulatory element in the release of different hormones [2]. From recent experimental data, however, it has become clear that the picture is more complex, because the connection is reciprocal, the gonadal hormones are also influencing the GABA system: they modulate the GABA levels and GABA receptors in several brain areas [3–5] and induce plastic changes in GABAergic synapses [6].

Our earlier quantitative post-embedding immunocytochemical analysis of the arcuate nucleus revealed that the administration of a single dose of 17β-estradiol resulted in a significant decrease in the number of GABA-immunoreactive axo-somatic synapses in ovariectomized rats [7]. It also indicated that there is a continuous synaptic remodeling in the arcuate nucleus during the estrus cycle, which is driven by the changing 17β-estradiol levels in the plasma [8].

The estradiol-induced synaptic remodelling may have functional consequences and we wanted to gain further insight into its physiological significance. To address this question the aims of the present studies were to investigate whether the 17β-estradiol-induced decrease in inhibitory synaptic inputs on the arcuate neurons results in a change in their electrophysiological activity, and to study the possible effects of activation of the olfactory and somatosensory systems on the activity of the neurons in the arcuate nucleus.

Materials and Methods

Surgical procedures: The experimental procedures used in this study followed the protocol for animal care approved by both the Hungarian Health Committee (1998) and the European Communities Council Directives (86/609/EEC). Three-month-old anesthetized ovariectomized rats (27 animals) were secured in a stereotaxic headholder (David Kopf) that provided access to the arcuate nucleus. During the experiments, the rats were anesthetized with a mixture of Ketavet (10.0 mg/100 g) and Rompun (xilasine, 0.8 mg/100 g). After surgery the animals were allowed to rest for 1 h. The core temperature was maintained at 37°C. During the course of the experiments, while the activity of an arcuate neuron was recorded (at least 25–30 min), 17β-estradiol was injected (100 μg/100 g in sesame oil, i.p.). Five minutes after the injection the plasma concentration of

estradiol reached 60–120 pg/ml and at the completion of the experiments the values were between 150 and 250 pg/ml, which is above the physiological levels measured in intact females at the time of the proestrus morning peak. According to our experimental paradigm one arcuate cell was studied per animal.

Stimulation and recording: The possible effects of electrical stimulation of the vibrissa pad and/or accessory olfactory bulb (AOB) on the activity of the neurons in the arcuate nucleus were also tested. The whisker pad was stimulated with bipolar needle electrodes (1 Hz, 0.3 ms duration, 150–200 μA), while the AOB was stimulated with bipolar tungsten electrodes (2 Hz, 0.3 ms duration, 50–100 μA) at the following coordinates: 5 mm anterior to the bregma and 1.4 mm lateral to the midline. With the aid of stereotaxic guidance, unit discharges in the arcuate nucleus were recorded extracellularly with glass micropipets filled with 2.5 M NaCl (impedance 15–20 MΩ). The electrodes were advanced in 3–5 μm steps, by means of a Narishige hydraulic micromanipulator. The signals were fed into a differential amplifier with 1 Hz lower and 10 kHz upper frequency limits, and visualized on a Tektronix storage oscilloscope. Amplified unit responses were fed into a computer via an interface (Digidata 1200, pClamp 6.0.4. software, Axon Instruments) and stored for further processing.

After the experiments the animals were fixed by transcardial perfusion by 4% paraformaldehyde in 0.1 M phosphate buffer. The brains were removed and site of the recording electrode was verified in cresyl violet-stained Vibratome sections.

Results

The *in situ* study of the electrophysiological activity of the arcuate neurons is not an easy task in the mouse [9] and it is even more difficult in the rat: this is one of the possible reasons why *in vitro* recording is frequently used in such studies [10,11]. Considering the complex synaptic organization of the hypothalamus and the arcuate area, this technique has serious limitations, because the slice preparation lacks functionally important input and output connections. The only way to study the effect of certain sensory inputs and systemically administered 17β-estradiol on the activity of arcuate neurons is *in situ* recording; therefore in the present paper we used this technique. In the course of our experiments, we measured the activity of more than 30 units, and analysed the data when the unit activity could be followed for ⩾ 25–30 min.

The effect of 17β-estradiol on the activity of the arcuate neurons: In all those cases when unit activities could be followed for a sufficient time, spontaneous activity of the neurons increased after 20–25 min of 17β-estradiol application. At the 25th minute the difference was highly significant: the frequency was increased from 5.5 ± 1.8 spikes/s (mean ± s.d.) to 20.2 ± 2 spikes/s (Fig. 1). In the same experiments we tested the effect of different modulatory components on the activity of arcuate neurons. Four of the nine neurons responded to whisker pad stimulation, exhibiting enhanced activity on somatosensory inputs (Fig. 2). The increased

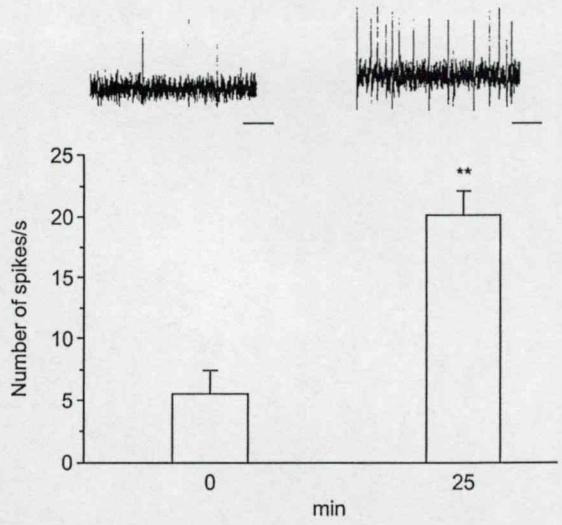

FIG. 1. Spontaneous activity of arcuate neurons before (0 min) and after (25 min) 17β-estradiol injection. Inset: Activity of an arcuate neuron before and 25 min after 17β-estradiol treatment. Bar = 100 ms. ** $p < 0.01$.

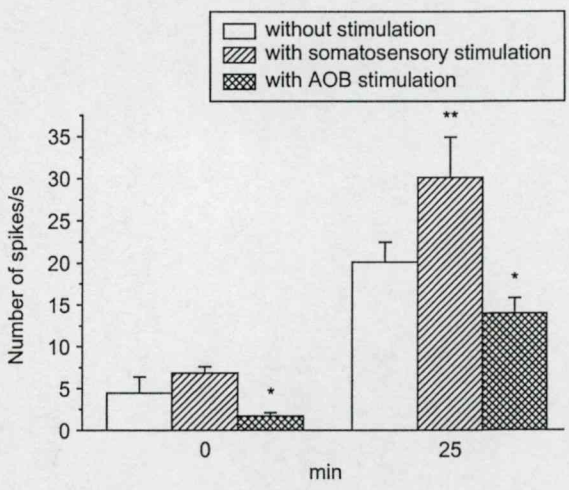

FIG. 2. The modulatory effect of vibrissa pad (hatched columns) and accessory olfactory bulb (crosshatched columns) stimulation on the spontaneous activity of arcuate neurons before (0 min) and after (25 min) 17β-estradiol injection (i.p.). * $p < 0.05$, ** $p < 0.01$.

firing was observed both before and after 17β-estradiol application (7 ± 0.8 spikes/s and 30.3 ± 4.7 spikes/s, respectively). AOB stimulation, however, which was tested on the same cells, resulted in an opposite effect, with decreased activity in both the absence and presence of 17β-estradiol. In control circumstances the firing frequency changed from 4.6 ± 1.8 to 1.9 ± 0.3 spikes/s, while after 17β-estradiol treatment the values were 20.2 ± 2.3 and 14.1 ± 1.9 spikes/s: the differences in both cases were significant (Fig. 2).

Discussion

The results clearly show that i.p. injection of 17β-estradiol is able to significantly increase the activity of the arcuate neurons within 20–25 min. Our data are in agreement with earlier findings which indicated that a number of steroid hormones exert marked electrophysiological effects in the CNS [12]. Concerning the sites and mechanisms of hormone actions, however, conflicting opinions are existing on the hypothesis if genomic or non-genomic factors play a role in this phenomenon. Many of the effects are believed to be mediated by interactions with intracellular receptors that result in gene-controlled changes in protein synthesis [13], but on the other hand they are often interpreted as direct membrane effects of hormones. The main argument in favor of the direct effect is the fast onset of action of the steroid observed in slice preparations, but these data are also contradictory. Li *et al.* [9] reported increased activity but found no difference between estrogen-treated and control animals for any of the electrophysiological characteristics which should reflect a change in excitability of neurons. Yeoman and Jenkins [14] demonstrated that the arcuate neurons maintained their diurnal pattern of activity (i.e. increased firing rate during proestrus afternoon) in slices if the animals were pretreated with estrogen. These data can not be explained as a direct membrane effect of estrogen they rather indicate that estrogen might act on other parts of the brain, thereby increasing the amount of excitatory information transmitted to the arcuate neurons.

In their experiments, Li *et al.* [9] and Yeoman and Jenkins [14] used slice preparation from animals that were chronically treated with estradiol; therefore they have no data about the time course of the estradiol effect. This information, however, is very important for the understanding of the possible molecular mechanisms and the result of our *in situ* experiments show that the enhanced activity of arcuate neurons occurs within 25 min.

Although the mechanism of the effect of intraperitoneally applied estrogen on the arcuate neurons is still obscure, some genomic effects of steroids can be very rapid. According to Mosher *et al.* [15], it can be within the range of 10 or 20 min, i.e. the 20–25 min latency reported here can be explained by this mechanism [16]. After 5 min of i.p. injection the estradiol concentration in the plasma reaches a level which is higher than that of following the proestrus morning surge. This concentration is maintained for a prolonged period and it was also shown that the circulating estradiol is delivered to the target cells in a few minutes. The fact that during the phases of increased neuronal firing Garcia-Segura *et al.* [17] demonstrated increased gene transcription and nucleo-cytoplasmic transport may also indicate genomic action. According to our working hypothesis estradiol acts on the GABAergic system and the observed increase in activity is the consequence of the disinhibition of arcuate neurons.

We have found that the majority of the evaluated units did not respond to different sensory stimuli. There is a population, however, in which the spontaneous activity could be influenced by stimulation of both the somatosensory and the olfactory systems i.e. these cells are receiving inputs from both directions. Although Li *et al.* [9] found that the AOB acts to enhance the activity of a subpopulation of arcuate neurons, and that neural transmission could be modulated by estrogen, as far as we know, our observation is the first demonstration of the modulatory effect of trigeminal activation on arcuate neurons. The two types of sensory modulation resulted in different effects, the AOB and whisker pad stimulation caused a decreased and increased firing, respectively. The somatosensory and olfactory stimuli are important in the sexually differentiated behavioral and neuroendocrine functions; therefore further studies are needed to elucidate the role of arcuate neurons in processing these inputs.

Conclusion

Twenty-five minutes after the i.p. administration of 17β-estradiol we recorded a significant increase in the spontaneous activity of arcuate nucleus neurons. In the present study we used an *in situ* preparation, i.e. all the synaptic connections of the cells remained intact and we were able to follow the development of the hormonal effect on the same units. The late onset of the estradiol action makes it unlikely that the changes are the consequence of direct membrane effect and we propose that the enhancement of firing is the result of the decrease in inhibitory synaptic inputs on arcuate neurons. We could demonstrate that somatosensory (trigeminal) and olfactory inputs are also modulating the activity of these neurons.

References

1. Adler BA and Crowler WR. *Endocrinol* **118**, 91–97 (1986).
2. Decavel C and Van Den Pol AN. *J Comp Neurol* **316**, 104–116 (1992).
3. Maggi A and Pérey J. *J Neurochem* **47**, 1793–1799 (1986).
4. Majewska MD, Demirgoren S and London ED. *Eur J Pharmacol* **189**, 307–315 (1990).
5. Lambert JJ, Belelli D, Hill-Venning C *et al. Cell Mol Neurobiol* **16**, 155–174 (1996).
6. Parducz A, Pérez J and Garcia-Segura LM. *Neuroscience* **53**, 395–401 (1993).
7. Garcia-Segura LM, Chowen JA, Parducz A *et al. Prog Neurobiol* **44**, 279–307 (1994).
8. Olmos G, Naftolin F, Pérez J *et al. Neuroscience* **32**, 663–667 (1989).
9. Li CS, Kaba H, Saito H *et al. Neuroscience* **29**, 201–208 (1989).
10. Nishihara M and Kimura F. *Neuroendocrinol* **49**, 215–218 (1989).
11. Lagrange AH, Ronnekleiv OK and Kelly MJ. *J Neurosci* **14**, 6196–6204 (1994).
12. Orsini JC, Barone FC, Armstrong DL *et al. Brain Res Bull* **15**, 293–297 (1985).
13. McEwen BS, Krey L and Luine V. *Res Publ Assoc Res Nerv Ment Dis* **56**, 255–268 (1978).
14. Yeoman RR and Jenkins AJ. *Neuroendocrionol* **49**, 144–149 (1989).
15. Mosher K, Young D and Munck A. *J Biol Chem* **246**, 264–259 (1971).
16. McEwen BS, Coirini H and Schumacher M. Steroid effects on neuronal activity: when is the genome involved? In: Chadwick D and Widdows K, eds. *Steroids and Neuronal Activity*. Chichester: John Wiley and Sons, 1990: 3–21.
17. Garcia-Segura LM, Luquin S, Martinez P *et al. Devl Brain Res* **73**, 63–70 (1993).

ACKNOWLEDGEMENTS: The work was supported by grants from OTKA (T 022280 and T 029979).

Received 23 August 1999; accepted 23 September 1999